UNIVERSITY OF BIRMINGHAM

Research at Birmingham

The histone-deacetylase-inhibitor suberoylanilide hydroxamic acid promotes dental pulp repair mechanisms through modulation of matrix metalloproteinase-13 activity

Duncan, Henry; Cooper, Paul; Smith, Anthony; Fleming, Garry James P.; Partridge, Nicola C.; Shimizu, Emi; Moran, Gary P.

Link to publication on Research at Birmingham portal

Journal of Cellular Physiology

The histone-deacetylase-inhibitor suberoylanilide hydroxamic acid promotes dental pulp repair mechanisms through modulation of matrix metalloproteinase-13 activity

SCHOLARONE™
Manuscripts

ORIGINAL RESEARCH ARTICLE

The histone-deacetylase-inhibitor suberoylanilide hydroxamic acid promotes dental pulp repair mechanisms through modulation of matrix metalloproteinase-13 activity

Henry F. Duncan[1], Anthony J. Smith[2], Garry J. P. Fleming[3], Nicola C. Partridge[4], Emi Shimizu[4], Gary P. Moran[5], Paul R. Cooper[2]

[1] Division of Restorative Dentistry & Periodontology, Dublin Dental University Hospital, Trinity College Dublin, Lincoln Place, Dublin 2, Ireland
[2] Oral Biology, School of Dentistry, University of Birmingham, Birmingham, B4 6NN, UK
[3] Material Science Unit, Dublin Dental University Hospital, Trinity College Dublin, Ireland
[4] Department of Basic Science and Craniofacial Biology, New York University College of Dentistry, USA
[5] Division of Oral Biosciences, Dublin Dental University Hospital, Trinity College Dublin, Ireland

Running head: HDACi promotes mineralization by modulating MMP-13 expression

Corresponding author: Henry F. Duncan; Division of Restorative Dentistry & Periodontology, Dublin Dental University Hospital, Trinity College Dublin, University of Dublin, Lincoln Place, Dublin 2, Ireland
Tel.: +353 (1) 612 7356; Fax: +353 (1) 612 7297; Email: Hal.Duncan@dental.tcd.ie

Keywords:
- **Histone-deacetylase-inhibitor**
- **Epigenetics**
- **Matrix metalloproteinase**
- **Cellular differentiation**,
- **Mineralization**
- **Gene expression**

Total number of text figures: seven   **Total number of tables**: seven

1

Abstract

Direct application of histone-deacetylase-inhibitors (HDACis) to dental pulp cells (DPCs) induces chromatin changes, promoting gene expression and cellular-reparative events. We have previously demonstrated that HDACis (Valproic acid, Trichostatin A) increase mineralization in dental papillae-derived cell-lines and primary DPCs by stimulation of dentinogenic gene expression. Here, we investigated novel genes regulated by the HDACi, suberoylanilide hydroxamic acid (SAHA), to identify new pathways contributing to DPC differentiation. SAHA significantly compromised DPC viability only at relatively high concentrations (5μM); while low concentrations (1μM) SAHA did not increase apoptosis. HDACi-exposure for 24h induced mineralization-per-cell dose-dependently after 2 weeks; however, constant 14d SAHA-exposure inhibited mineralization. Microarray analysis (24h and 14d) of SAHA exposed cultures highlighted that 764 transcripts showed a significant >2.0-fold change at 24h, which reduced to 36 genes at 14d. 59% of genes were down-regulated at 24h and 36% at 14d, respectively. Pathway analysis indicated SAHA increased expression of members of the matrix metalloproteinase (MMP) family. Furthermore, SAHA-supplementation increased MMP-13 protein expression (7d, 14 d) and enzyme activity (48h, 14d). Selective MMP-13-inhibition (MMP-13i) dose-dependently accelerated mineralization in both SAHA-treated and non-treated cultures. MMP-13i-supplementation promoted expression of several mineralization-associated markers, however, HDACi-induced cell migration and wound healing were impaired. Data demonstrate that short-term low-dose SAHA-exposure promotes mineralization in DPCs by modulating gene pathways and tissue proteases. MMP-13i further increased mineralization-associated events, but decreased HDACi cell migration indicating a specific role for MMP-13 in pulpal repair processes. Pharmacological inhibition of HDAC and MMP may provide novel insights into pulpal repair processes with significant translational benefit.

2

Introduction

The balance between the cellular enzymes, histone deacetylases (HDACs) and histone acetyltransferases (HATs), controls chromatin conformation and regulates transcription. Predominant HDAC activity results in the removal of acetyl groups from the histone tails within the nucleosome, leading to a condensed chromatin conformation and reduced transcription, while HAT activity has the opposite effect leading to an open, transcriptionally active chromatin structure (Bolden et al., 2006). There are 18 identified mammalian HDACs, which are categorized into four classes functioning via zinc-dependent or independent mechanisms (Gregoretti et al., 2004). Class I (-1, -2, -3, -8) are zinc-dependent, ubiquitously distributed and expressed in the cell nucleus (Marks and Dokmanovic, 2005), while class II (-4, -5, -6, -9, -10) are also zinc-dependent, but demonstrate tissue-restricted expression and shuttle between the nucleus and cytoplasm (Verdin et al., 2003; Marks, 2010). Class III HDACs, known as sirtuins, are not zinc-dependent, instead requiring coenzyme nicotinamide adenine dinucleotide (NAD+) for function (Haigis and Guarente, 2006), while there is currently only one class IV member, HDAC -11 (Villagra et al., 2009). A recent analysis of HDAC expression in human dental pulp tissue demonstrated that HDAC-2 and -9 were expressed in some pulp cell populations and strongly expressed in odontoblasts, the formative cells for mineralized dentin, while HDAC-1, -3 and -4 were only relatively weakly expressed within pulp tissue (Klinz et al., 2012), highlighting the tissue-specific expression of class I and II of HDAC.

Histone deacetylase inhibitors (HDACi) are epigenetic-modifying agents that alter the homeostatic enzyme balance between HDACs and HATs leading to an increase in acetylation and transcription. The increased gene expression induces pleiotropic cellular effects, altering cell growth (Marks and Xu, 2009), increasing cell differentiation (Schroeder and Westendorf, 2005), reducing inflammation (Shuttleworth et al., 2010) and modulating stem cell lineage commitment (Mahmud et al., 2014). A range of natural and synthetic HDACi, including valproic acid (VPA), butyric acid, trichostatin A (TSA) and suberoylanilide hydroxamic acid (SAHA), have been investigated with SAHA being the

3

first HDACi to gain United States Food and Drug Administration (FDA) approval for anti-cancer treatment (Grant et al., 2007). Increasingly, the positive transcriptional effects of HDACi are also being investigated in fields such as bone engineering (De Boer et al., 2006), and organ regeneration (de Groh et al., 2010). Traditionally, pan-HDACi (such as VPA, TSA and SAHA), which are active against Class I and II HDACs, have been investigated experimentally (Schroeder et al., 2007; Marks, 2010; Jin et al., 2013).

Within dental pulp research, a range of HDACis have been demonstrated to promote differentiation and increase mineralization dose-dependently, in both a dental-papilla derived cell-line (Duncan et al., 2012; Kwon et al., 2012) and primary dental pulp cell (DPC) populations at relatively low concentrations (Duncan et al., 2013; Jin et al., 2013; Paino et al., 2014). An HDACi-induced expression of specific dentinogenic-marker genes was demonstrated, which may drive the increase in mineralization (Duncan et al., 2012; Kwon et al., 2012). Other studies have identified the down-regulation of specific class I HDACs, -3 (Jin et al., 2013) and -2 (Paino et al., 2014) in mineralizing pulp cells. At present, no study has characterized the transcript regulation and novel pathways responsible for the HDACi-induced promotion of pulp mineralization using high-throughput approaches.

The matrix metalloproteinases (MMPs) are a family of host-derived zinc-dependent endopeptidases (Nagase and Woessner Jr, 1999). MMPs can not only degrade practically all proteinaceous extracellular matrix components (Verma and Hansch, 2007), but are also an important link to a host of tissues processes including angiogenesis, differentiation and chemotaxis by improving the bioavailability of growth factors through cleavage (Hannas et al., 2007; Borzi et al., 2010). MMPs have been shown to be central to normal and pathological remodelling processes in various mineralization-associated tissues, including bone (Paiva and Granjeiro, 2014), cartilage (Krane and Inada, 2003) and periodontal tissues (Ravanti et al., 1999). Recently, certain MMPs have generated significant interest within restorative dentistry with MMP-2 being identified in increased quantity in defensive reactionary dentine (Charadram et al., 2012) while MMP-13 (collagenase-3) expression increased during dental wound reparative processes (Suri et al., 2008; Yoshioka et al., 2013).

4

From a translation perspective, the identification of regulators that control lineage commitment and differentiation is paramount to the development of cell-based regenerative strategies. A complex HDAC-mediated control of bone remodelling and repair processes is emerging involving intricate epigenetic-control of a series of pathways (Bradley et al., 2011). MMP-13 activity may be particularly important in this process as it demonstrates relatively high expression in pulp tissue (Palosaari et al., 2003; Sulkala et al., 2004), has increased expression during mineralization (Winchester et al., 1999; Suri et al., 2008) and repressed-transcription by HDAC-4 in an mineralizing osteoblastic cell-line (Shimizu et al., 2010). Notably, microarray studies have demonstrated an HDACi-induced modulation of MMPs in mineralizing bone-derived cell cultures (Schroeder et al., 2007). Here for the first time, we investigate whether the clinically-approved HDACi, SAHA, could induce regenerative processes in primary DPC cultures with high-throughput transcriptional analyses being undertaken to identify novel genes and potential pathways activated. As transcriptomic analysis identified a significant role for several MMPs in the pulp reparative process; a subsequent aim of this study was to analyse the specific novel role of MMP-13 and its interaction with HDACi in modulating regenerative events in DPC cultures.

Materials and methods

Primary cell isolation and culture. Primary DPCs were isolated from the extirpated pulp tissue of freshly extracted rodent incisor teeth using enzymatic disaggregation (Patel et al., 2009). Briefly, teeth were dissected from male Wistar Hannover rats aged 25-30 days and weighing 120-140 g. Pulp tissue was extirpated, minced and transferred into Hank's balanced salt solution (Sigma-Aldrich, Arklow, Ireland) prior to incubation at 37°C, 5% CO_2 for 30 min (MCO-18AC incubator, Sanyo Electric, Osaka, Japan). Cells were transferred to an equal volume of supplemented α-MEM (Biosera, East Sussex, UK) containing 1% (w/v) penicillin/streptomycin (Sigma-Aldrich) and 10% (v/v) foetal calf serum (FCS) (Biosera). Single cells were obtained by passing through a 70 µm cell sieve (BD Biosciences) prior to centrifugation and re-suspension in 1 ml supplemented α-MEM. DPCs were expanded under standard culture conditions to passage 2 for use in all subsequent experiments.

5

Pharmacological inhibitor preparation. A 5 mM stock solution of the HDACi, SAHA (*N*-hydroxy-*N'*-phenyl-octanediamide) (Sigma-Aldrich), in dimethyl sulfoxide (DMSO) was diluted in phosphate buffered saline (PBS) (Sigma-Aldrich) prior to further dilution to experimental concentrations (0.25 µM - 5 µM) with supplemented α-MEM. A 5 mM stock solution of the MMP-13 specific inhibitor (MMP-13i) (Pyrimidine-4,6-dicarboxylic acid, *Bis*-[4-fluoro-3-methyl-benzylamide]) (Santa Cruz Biotechnologies, Heidelberg, Germany) in dimethyl sulfoxide (DMSO) was diluted to experimental concentrations (0.5 µM - 10 µM) in supplemented α-MEM.

Cell growth and viability analysis. DPCs were initially seeded 1 x 10^5 cells per well [6-well plates (Sarstedt, Wexford, Ireland)] for 72 h. For experimental day 0, cells were cultured in supplemented α-MEM for a further 24 h prior to harvest. SAHA (0.25, 0.5, 1, 3 and 5 µM) was added to the supplemented α-MEM at day 0. Control samples did not contain SAHA supplementation. Trypan blue (Sigma-Aldrich) staining (n=4) was used to assess cell viability. Thereafter 1 and 2 µM MMP-13i alone or in combination with SAHA were assessed for effects on DPC growth and viability under mineralizing conditions. Cells were seeded as previously described and at 72 h (experimental day 0), mineralizing medium (supplemented α-MEM including 50 µg/ml ascorbic acid, 0.1 µM dexamethasone and 10 mM β-glycerophosphate) was applied for a further 1 and 4 days. As 24 h HDACi culture had previously been demonstrated in induce mineralization at 14 days (Duncan et al., 2013), SAHA (1 µM) was added to the mineralizing medium, at day 0, for the initial 24 h only, while the MMP-13i was supplemented in cultures throughout. In the 5 day group, the SAHA/MMP-13i-supplemented mineralizing medium was replaced after 24 h with MMP-13i-supplemented mineralization media for a further 4 days. Control cultures were in mineralizing medium either without HDACi or MMP-13i. Three independent experiments (n=3) were performed in triplicate for time points and combinations of SAHA and 1 µM, 2 µM MMP-13i, respectively.

6

Live-Dead staining assay. DPCs were seeded at a density of 5×10^3 in clear bottom black 96-well plates (Corning, NY, USA) for 24 h. At 24 h (experimental day 0), the cells were cultured in mineralizing medium for 24 or 48 h (experimental day 1 and 2) prior to harvest. SAHA (0.25, 0.5, 1, 3 and 5 μM) was added to the medium at day 0. Control cultures contained mineralization α-MEM without SAHA, while 1% saponin (Sigma-Aldrich) was applied for 10-15 min to verify cell death. At experimental end-points, cultures were washed twice in PBS prior to incubation with Live/Dead™ reagents, 4 μM ethidium homodimer-1 (EthD-1) and 2 μM calcein AM (Life Technologies, Paisley, UK) (Murphy et al., 1998). Fluorescent signals were quantified spectrophotometrically (Tecan Genios Spectrophotometer, Unitech, Dublin, Ireland). Four independent experiments (n=4) were performed in triplicate for each HDACi concentration.

Flow cytometry (FC). FC detection (BD FACSCanto II, BD Biosciences) of annexin V (AV) binding and propidium iodide (PI) staining (Annexin V-FITC Kit, BD Bioscience) was performed to assess viability and apoptosis. Cells (1×10^5 per well in 6-well plates) were cultured in supplemented α-MEM for 24 h, prior to addition of SAHA (1 μM) for a further 24 h. The experimental SAHA concentration and 24 h time point was selected from the results of the cell growth, live/dead and mineralization assays and represented the end of the DPCs exposure to the HDACi. Untreated cells in supplemented α-MEM served as the negative control and cells in supplemented α-MEM with 6 μM camptothecin (Sigma-Aldrich) were used as a positive control to confirm apoptosis. Cells were detached (trypsin/EDTA), washed twice with PBS and suspended in a 1 x AV binding buffer (BD Bioscience). A 100 μl aliquot of the cell suspension (1×10^5) was incubated at room temperature with 5 μl FITC-AV and 5 μl PI for 15 min. Thereafter, 400 μl of 1 x AV binding buffer was added and cells analysed by FC within 1 h. Excitation was performed at 488 nm and the emission filters used for AV-FITC and PI were 530/530 nm and 585/545 nm, respectively. Data were analysed using FC software (FloJo, Tree Star, OR, USA) and the PI staining

7

intensity plotted against FITC intensity. Four independent experiments (n=4) were performed with 10,000

cell events measured for each experimental/control group.

Mineralization assays. Cells were seeded (5×10^4 per well in 6-well plates) and cultured in supplemented

α-MEM for 72 h. At 72 h (day 0), DPCs were supplemented with mineralizing medium with SAHA

(0.25, 0.5, 1, 3 and 5 μM) for the initial 24 h or for 14 days. In the 24 h HDACi-exposure cultures,

SAHA-supplemented mineralizing medium was removed after 24 h, prior to culture with an HDACi-free

mineralizing medium for a further 13 days, while in the 14 day HDACi-exposure samples SAHA

supplemented the mineralizing medium throughout. The 14 day time-point was selected as rat DPCs in

mineralizing culture require this time to secrete mineral that can be discriminatively measured

quantitatively by alizarin red staining (Duncan et al., 2013). Control samples were in mineralizing

medium without SAHA with medium changes every 3 days. For analysis, cultures were washed 3 times

for 5 minutes in PBS and fixed in 10% formaldehyde for 15 min, washed with distilled water and finally

stained with 1.37% (w/v) alizarin red S (Millipore, Cork, Ireland) (pH 4.2) for 15 min at room

temperature. Excess stain was removed by washing with distilled water; the residual stain was solubilised

in 10% (v/v) acetic acid (Millipore). Stain intensity was quantified spectrophotometrically at 405 nm

(Gregory et al., 2004) (Tecan Genios Spectrophotometer, Unitech). Mineral production per cell data for

all concentrations of SAHA were subsequently calculated based on parallel experiments whereby viable

cells were counted following Trypan blue staining. Four independent mineralization and cell count

experiments (n=4) were performed in triplicate for both 24 h and 14 day SAHA exposures, respectively.

To assess the effects of 1 and 2 μM MMP-13i +/- SAHA on DPC mineralization, a similar

protocol to that described above was applied. At 72 h, the DPCs were cultured (day 0) in a mineralizing

medium with the addition of MMP-13i (1 μM or 2 μM) alone or in combination with 1 μM SAHA. DPCs

were cultured with SAHA for only the initial 24 h, prior to culture with an HDACi-free mineralizing

medium for a further 13 days, while MMP-13i was supplemented in cultures for the 14 day experimental

period. The control samples contained DPCs cultured in mineralizing medium in the presence and absence of SAHA. Three independent experiments (n=3) were performed in triplicate for all combinations of SAHA and MMP-13i, respectively**.**

RNA, cDNA and labelled cRNA preparation. Cells were seeded (6 x 10^4 cells per well) in a 6-well culture dish in supplemented α-MEM for 72 h. At 72 h (experimental day 0), cells were either cultured for 24 h in supplemented mineralizing medium containing 1 µM SAHA prior to harvest (24 h samples) or incubated with an HDACi-free mineralizing medium for a further 13 days (experimental day 14). Medium was changed every 3 days in the 14 days group. Control samples contained cells cultured in mineralizing medium without SAHA. Cultures were detached (trypsin/EDTA), homogenized [T10 basic S2-Ultra-Turrax tissue disrupter (IKA, Staufen, Germany)] and RNA extracted using the RNeasy mini kit (Qiagen, West Sussex, UK)and quantified spectrophotometrically (Nanodrop 2000, Thermo Fisher Scientific). For microarray samples, a 75 ng aliquot of total RNA was labelled with Cyanine 3-CTP or Cyanine 5-CTP using the Two-Color Low Input Quick Amp labeling Kit (Agilent Technologies, Cork, Ireland) according to the manufacturer's instructions. Briefly, RNA was converted to cDNA with an oligo dT-promoter primer and Affinity-Script-RT (Agilent Technologies), prior to experimental/control groups being labelled with Cy5 or Cy3 and transcribed to cRNA (Agilent Technologies). The labelled and amplified cRNA was purified as previously described using the RNeasy mini kit (Qiagen) and Cy3, Cy5 concentration, RNA absorbance 260/280 nm and cRNA concentrations determined spectrophotometrically (Nanodrop 2000, Wilmington, DE, USA). This enabled specific activity and target yields to be calculated prior to microarray experimentation.

Gene expression microarray and data analysis. The Agilent 4 x 44k v3 whole rat genome oligonucleotide gene expression microarray (Agilent Technologies) was used to analyse the transcript profiles of SAHA treated (1 µM) and untreated DPC cultures at both 24h and 14 days. The microarray analyses were

9

performed on quadruplicate independent DPC cultures (n=4) at both time-points. A total of 825 ng of

labelled cRNA from each sample (treated and untreated) was loaded onto an individual array according to

the manufacturer's instructions and co-hybridised at 65°C for 17 h, washed and scanned in GenePix-

Personal 4100A, Pro 6.1 (Axon, Molecular Devices, CA, USA) at a resolution of 5 μm. Raw data were

exported to GeneSpring GX12 and signals for each replicate spot were background corrected and

normalized using Lowess transformation. Log_2 fluorescent intensity ratios were generated for each

replicate spot and averaged. Genes that were differentially expressed (>2.0 fold) in the SAHA group

relative to control were identified after passing a t-test (p<0.05), post-hoc test (Storey with Bootstrapping)

with a corrected q value of 0.05. Genes in the expression data sets were first 'ranked' based on Log_2

values from highest to lowest for both groups at both time points, prior to hierarchical clustering being

used to group gene expression in each condition using the default settings in Genespring GX12. Gene

Ontology (GO) was evaluated using Go-Elite (http://www.genmapp.org/go_elite) (Salomonis et al.,

2009), which is designed to identify a minimal non-redundant set of biological Ontology terms or

Pathways to describe a particular set of genes or metabolites. Subsequent pathway analysis was

undertaken using Pathvisio (http://www.pathvisio.org/) (van Iersel et al., 2008; Kelder et al., 2012), which

uses an over-representation analysis, only reporting on GO terms and pathways with a z score >2, a

permutation p<0.01, and three or more regulated genes for the pathway. Microarray data have been

submitted to Gene Expression Omnibus (GEO), accession number: GSE67175.

cDNA synthesis and quantitative RT-PCR analysis. For quantitative validation, DPCs were cultured and

harvested at 24 h and 14 days in an identical protocol to microarray analysis above. MMP-13i

supplemented cultures were harvested at 24 h and 5 days. Briefly, at experimental day 0 (72 h), the cells

were cultured in supplemented mineralizing medium containing 2 μM MMP-13i and harvested at 24 h

and 5 days. Two control groups contained cells cultured in mineralizing medium in both the presence and

absence of 24 h 1 μM SAHA. This time point coincided with both the SAHA microarray data and the

MMP-13i cell growth study. RNA was isolated as described above, converted to single-stranded cDNA

10

using the TaqMan™ reverse transcriptase kit and 50 µM random hexamers (Life Technologies), prior to cDNA concentrations being determined spectrophotometrically at 260 nm (Nanodrop 2000, Thermo Fisher Scientific).

The q-RT-PCR analysis was performed for rat genes using specific primers (Invitrogen, Life Technologies, Thermo Scientific, Paisley, UK). The primer sequences, product sizes and the accession number are listed in Table 1. Synthesised cDNA was amplified in a reaction containing; 12.5 µl SYBR Green Fast PCR reagent (Applied Biosystems), 1 µl Forward /Reverse primer, 8 µl DEPC-treated water and 100 ng of template cDNA. PCRs were performed using the Applied Biosystems 7500 Fast Real-Time PCR thermal cycler (Applied Biosystems) and subjected to a designated number of amplification cycles (40 cycles), where a typical cycle was 95°C for 3 secs and 60°C for 30 secs. Real-time PCR data were normalized to β-actin, and fold change in gene expression was obtained using the formula $2^{((Ct_{ctrl} - Ct_{\beta\text{-actin}}) - (Ct_{exp} - Ct_{\text{-actin}}))}$, where Ct is the threshold cycle, ctrl is the control and exp is the experimental samples. Four independent experiments (n=4) were performed for each target gene in triplicate at both 24 h and 14 days to validate the microarray data. Three independent experiments (n-3) were carried out in triplicate for the MMP-13i experimental gene targets.

Enzyme-Linked Immunosorbent Assay (ELISA). Cells were seeded (6×10^4 per well) in 6-well plates and cultured in supplemented α-MEM for 72 h. At 72 h, the DPCs were cultured (day 0) in a mineralizing medium with addition of 1 µM SAHA for the initial 24 h of culture. Cells were harvested at experimental days 1, 7, 14, and 21 for analysis. The HDACi-supplemented mineralizing medium was removed after 24 h prior to culture with an HDACi-free mineralizing medium for a further 6, 13 or 20 days. The quantification of the MMP-13 protein was investigated at 3 time-intervals, prior to the 21 day mineralization end point. Control culture samples did not contain SAHA supplementation. Subsequently, medium was aspirated and cultures washed twice in ice cold PBS (pH 7.4), prior to the addition of 300 µl lysis buffer containing mammalian protein extraction reagent (M-PER) (Thermoscientific Pierce,

11

Rockford, IL, USA) halt protease inhibitor (Thermoscientific Pierce) and 1 mM phenylmethylsulfonyl fluoride (PMSF) (Thermoscientific Pierce). A Bradford dye-binding method (Bio-Rad, Hemel Hempstead, Hertfordshire, UK) was used for normalisation. Total MMP-13 levels were analysed by quantitative sandwich ELISA technique (Cusabio, Wuhan, Hubei Province, China) according to the manufacturer's instructions and absorbance measured at 450 nm with the correction wavelength set at 570 nm. Results were calculated from a standard curve. Three independent experiments (n=3) were performed in triplicate for each experimental concentration and time interval.

MMP-13 Enzyme Activity Assay. The specificity of the MMP-13 inhibitor was determined by addition of 0 (control), 0.5, 1, 2, 5 and 10 μM MMP-13i to samples containing 100 ng/ml of recombinant MMP-9 and MMP-13, which was diluted in assay buffer to a final dilution ratio of 1:100 (AnaSpec, San Jose, CA). A 96-well plate format was used with the Sensolyte™ 490 MMP-13 fluorimetric assay kit as per the manufacturer's instructions (Anaspec). Zymogens or pro-MMP-9 and 13 were activated immediately prior to experimentation by incubation with 1 mM 4-aminopheylmercuric acetate (APMA) for 40 mins (MMP-13) and 1 hour (MMP-9) at 37°C. Diluted samples were incubated for 45 minutes in a black 96-well plate (Perkin Elmer, Waltham, MA, USA) prior to the fluorescent intensity being measured by a spectrophotometer (Tecan Genios Spectrophotometer) at 360 nM (excitation) and 465 nM (emission).

To measure MMP-13 activity in DPCs, cultures were seeded (6×10^4 cells per well) in a 6-well culture plate. At 72 h (experimental day 0), the cells were cultured for 24 h in supplemented mineralizing medium either containing 1 μM SAHA or 2 μM MMP-13i or a combination of both. Active MMP-13 activity was analysed at 2 time-points (48 h and 14 days) to reflect an early and late time point to coincide with the gene expression data. In the 48 h group and 14 day group, the HDACi-supplemented mineralizing medium was removed after 24 h prior to culture with an SAHA-free mineralizing medium for further 24 h or 13 days. In the MMP-13i samples the inhibitor supplemented the culture for the duration of the experiment. Two control groups consisting of supplemented α-MEM and supplemented

12

mineralizing medium. At the designated time-point, the medium was aspirated and the cell monolayer gently washed twice in ice cold PBS (pH 7.4), prior to the addition of 300 µl lysis buffer containing M-PER (Thermoscientific Pierce), halt protease inhibitor (Thermoscientific Pierce) and 1 mM PMSF (Thermoscientific Pierce). Harvested cells were collected. The Bradbury dye-binding method (Bio-Rad, Hemel Hempstead, Hertfordshire, UK) was used to equalize total protein concentrations in samples.

A 96-well plate format was used as before with the Sensolyte™ 490 MMP-13 fluorimetric assay kit according to the manufacturer's instructions (Anaspec). Briefly, the pro-MMP-13 zymogen was activated immediately prior to experimentation in all samples by incubation with 1 mM APMA for 40 mins at 37°C.   Fluorescent intensity was measured by a spectrophotometer (Tecan Genios Spectrophotometer) at 360 nM (excitation) and 465 nM (emission). For calculation of MMP-13 activity, each measurement was background-corrected to the average of the substrate controls. As the FRET substrate in the Sensolyte™ 490 MMP-13 kit can also be cleaved by MMP-1, -2, -3, -8, and -12 the MMP-13 specific inhibitor group was used to ascertain the effect of MMP-13 alone. Three independent experiments (n=3) were performed in triplicate for each experimental concentration at both time intervals.

Chemotaxis Transwell assay. To measure vertical DPC migration, 30 µl of supplemented α-MEM (without FBS) or control solutions were added into wells of a 96-well micro-chemotaxis plate with a 8 µm-pore size (NeuroProbe, Receptor Technologies, Warwick, UK) [43]. DPCs (3×10^4) were seeded in wells of the upper chamber. Test solutions examined supplemented α-MEM (without FBS) containing 1 and 3 µM SAHA, 1 and 2 µM MMP-13i and both 1 µm SAHA and 2 µM MMP-13i. DPCs in the SAHA test solutions were exposed to SAHA in culture for 3 h prior to seeding in the assay chamber. Control solutions included a negative control of supplemented α-MEM (without FBS) and a positive control of α-MEM medium containing 10% FCS. The micro-chemotaxis plate was incubated at 37°C in 5% CO_2 in air for 3 h to allow cell migration. Centrifugation was used to collect cells from the under-surface of the filter from the pores onto the bottom of the 96-well plate and 1mg/ml calcein AM (Life Technologies, Dun

13

Laoghaire, Ireland) was added to each well at a final dilution ratio of 1:250 for 30 minutes to label cells prior to fluorescence measurement with a spectrophotometer (Tecan Genios Spectrophotometer) at excitation 486 nM and emission of 540 nM. Readings were converted to cell numbers using standard curves of known cell numbers (Smith et al., 2012). Three independent experiments (n=3) were performed in triplicate for each experimental group.

Scratch wound healing assay. To assess horizontal migration, DPCs were seeded at a density of 6 x 10^4 in 6-well plates and cultured in supplemented α-MEM until confluent. Cells were starved for 24 h in supplemented α-MEM medium without FBS, prior to a carefully placed scratch wound being made through the confluent monolayer using light pressure and a 200μl pipette tip (0 h). DPCs were washed with PBS to remove cell debris and incubated with mineralizing medium in the presence and absence of 1 μM SAHA and 2μM MMP-13i for 24 h. At 0 h and 24 h, images of the scratched monolayer cultures were captured (Primovert, Carl Zeiss, Cambridge, UK). Data were quantified by measuring each wound closure area using ImageJ software (ImageJ, USA) and expressing as a percentage relative to the wound closure area in the control medium. Three independent experiments (n=3) were performed in triplicate for each experimental group.

Statistical Analyses. One-way analysis of variance (ANOVA) and Tukey's post-hoc tests were used for experiments to determine the influence of HDACi and MMP-13i concentration (p<0.05) on the cells using SigmaStat 14.0 software (SPSS, IL, USA). The statistical significance of the qRT-PCR data was assessed using Student's t-test. Microarray gene expression and pathway analysis were assessed as previously described.

Results

Short-term SAHA treatment promotes mineralization without loss of cell viability, while long-term SAHA inhibits differentiation. Previous dental pulp cell experimentation has shown that pan-HDACi (Trichostatin A and Valproic acid) can exert anti-proliferative effects at relative high concentrations, but at relatively low concentrations can promote mineralization dose-dependently (Duncan et al., 2012; Duncan et al., 2013). To investigate the cellular effects of SAHA (Grant et al., 2007), the effects of low doses of SAHA on primary DPC growth, viability, apoptosis and mineralization were investigated. While DPC numbers were decreased (reduced up to 45%) at 24 h by the higher experimental concentrations of 3 and 5 µM SAHA (p=0.012/p<0.001), compared with HDACi-free control cultures, at a SAHA concentration of 1 µM there was no significant effect on growth (Fig. 1A). Furthermore, cell viability investigated by both Trypan blue exclusion and live/dead staining demonstrated no significant loss of viability at 24 h (p>0.140/ p>0.275) at the low dose SAHA concentrations applied. A relatively small (~10%) but significant loss of viability at 5 µM SAHA was demonstrated by live/dead staining compared with the control at 48 h (p=0.003) (Fig. 1B). Consistent with previous HDACi experimentation (Duncan et al., 2013), 14 d mineralizing cultures exposed to an initial 24 h dose of SAHA, demonstrated significant dose-dependent increases in mineralization per cell at all concentrations >0.5 µM (p<0.046) applied, compared with HDACi-free control cultures (Fig. 1C). Notably, samples in which the HDACi was replenished every 3 days for the duration of the 14 d mineralization experiment demonstrated the opposite effect, with mineralization per cell inhibited at all concentrations >0.5 µM SAHA (p<0.013). This finding is supported by a recent *in vivo* animal study, which reported that the HDACi dosage regime may be as critical in promoting a positive mineralization response (Xu et al., 2013). From the growth, viability and mineralization data, 1 µM SAHA was selected for further flow cytometry (FC) and gene expression analysis as it was the highest mineralization promoting concentration not to induce DPC growth arrest at 24 h. Viable cell numbers data assessed by FC (Fig. 1D) were not significantly affected at 1 µM SAHA (p=0.058), while no significant increase in early or late apoptosis was detected following 24 h SAHA exposure (Fig. 1E-F).

15

SAHA significantly altered DPC gene expression at relatively early and late mineralization inducing time-points. To determine the molecular mechanisms whereby 1 μM SAHA accelerates mineralization effects, we performed microarray analyses. Based on previous work (Duncan et al., 2013), we hypothesized that 24 h SAHA treatment would reprogram gene expression at a relatively early time-point and accelerate the differentiation process up to 14 days. Subsequently, we isolated mRNA from primary DPCs cultured in mineralizing medium at 24 h, the end of SAHA exposure, and 14 d. At 24 h, of the 23,347 genes analysed, SAHA significantly increased the expression >2-fold of 314 transcripts and suppressed the expression of 450 genes, representing alteration of only 3.3% of the array oligonucleotides, while only 23 transcripts were similarly up-regulated and 13 down-regulated at 14 d (Fig. 2A and 2B). The top 40 SAHA most up- and down-regulated genes at 24 h are listed in Tables 2 & 3 and the top 20 up- and down-regulated genes at 14 d in Tables 4 & 5. The observed gene expression patterns demonstrate that although SAHA-induced transcriptional change, more genes were suppressed than induced at 24 h and the expression changes were of a relatively modest level. Notably, similar levels of differential gene expression have been reported in other HDACi high-throughput transcriptomic studies (Schroeder et al., 2007; Boudadi et al., 2013). Interestingly, although selected mineralization-associated transcripts are significantly upregulated only at 24 h (MMP-9, 2.99-fold; Adrenomdeullin, 3.4-fold), Ameloblastin was upregulated at 14 days only (1.72-fold) and MMP-13 at both time points (2.45-fold 24 h; 1.6-fold 14 d) (Fig. 2C).

SAHA-induced genes within the matrix metalloproteinase family and endochondral ossification related pathway in DPC s. To identify potential pathways that are affected by SAHA exposure in primary DPCs under mineralizing conditions, the microarray gene expression dataset was subjected to pathway analysis using Go-Elite and Pathvisio analysis software. Bioinformatic analysis indicated that the endochondral ossification pathway and the matrix metalloproteinase family (Fig. 2D) were significantly induced by

16

SAHA exposure in DPCs at 24 h (Table 6). Specifically, four up-regulated genes (MMP-9, 2.99-fold; MMP-13 2.45-fold; Ctsl1, 2.24-fold; Plat, 1.93-fold) playing critical roles in removal and organisation of extracellular matrix were identified. From this select group of genes, MMP-13 was of particular interest as it was previously reported that the Class II HDAC-4 repressed MMP-13 transcription in a mineralizing cell-line (Shimizu et al., 2010). Furthermore a potential role for MMP-13 in human pulp cell differentiation has been proposed (Suri et al., 2008; Yoshioka et al., 2013). As a result, a panel of 20 genes of interest, including MMP-13 and MMP-9, were selected for confirmatory qRT-PCR analysis (Table 1). A range of transcripts was selected based on their levels of differential regulation, their potential roles in mineralization processes and pathways (e.g endochondral ossification). The confirmatory analysis corroborated the microarray data (Table 7). Notably, at 24 h, SAHA-induced significant increases in MMP-9 (2.76-fold, p=0.011), MMP-13 (2.19-fold, p=0.043), as well as expression of several up-regulated mineralization genes which have been reported as significant markers of dental pulp mineralization, including Nestin (1.82-fold, p=0.005), IBSP (2.38-fold, p=0.005), BMP-4 (2.79-fold, p=0.015) and Adrenomedullin (3.06-fold, p=0.047) (Fig. 3A and 3B).

MMP-13 protein expression and enzyme activity are increased in mineralizing DPC cultures and further increased by low-dose SAHA. To further analyse the interaction of SAHA and MMP-13, DPCs were cultured under mineralizing conditions in the presence and absence of SAHA for 24 h, prior to HDACi-free incubation for up to 21 days. The aim of this time-course assay was to examine the expression and activity of MMP-13 protein during DPC proliferation, differentiation, and mineralization; it has previously been shown (Winchester et al., 1999; Suri et al., 2008) that MMP-13 expression increases during the DPC differentiation before reducing later during mineralization. The influence of HDACi on MMP-13 expression over the same time period has not been previously investigated. Overall in this study, MMP-13 protein expression, measured by quantitative ELISA, demonstrated a peak level at 7 days in all groups (supplemented medium, mineralizing medium, mineralizing medium/SAHA), which reduced at 14

17

days and returned at 21 days to baseline levels. Although there were no significant differences in MMP-13 protein levels at 24 h (p>0.728) in any group, by 7 days a significant increase was evident in mineralizing cultures in the absence (p=0.044) and presence of 1 µM SAHA (p=0.02), compared with non-mineralizing control cultures (Fig. 4A). The addition of SAHA to mineralizing cultures resulted in a significant increase in MMP-13 expression at 7 days compared with the mineralizing medium control (p=0.034). At 14 days, there was also a significant increase in the expression of MMP-13 protein levels for the SAHA samples, compared with both the supplemented medium group (p=0.03) and the mineralizing medium group (p=0.029). At the late mineralization stage of 21 days, there were no significant differences between any groups and MMP-13 expression returned to baseline levels.

To determine whether changes in active MMP-13 enzyme activity reflected increased gene and protein expression, we used a commercial fluorogenic activity assay and selective pharmacological inhibition to block MMP-13 activity. Experimental MMP-13i concentrations were established initially by reference to previously published studies (Toriseva et al., 2007; Nishimura et al., 2012; Lei et al., 2013). An *in vitro* experiment was also undertaken to confirm enzyme activity inhibition and specificity. MMP-13i resulted in an 87% reduction of MMP-13 activity at a concentration of 1 µM and 93% reduction at 2 µM (Fig. 4B), however, for all inhibitor concentrations >0.5 µM, activity was significantly reduced (p<0.0001). At the same concentrations the MMP-13i had no significant effect on MMP-9 activity (p=0.709) (Fig. 4B). Subsequently, a fluorogenic activity assay was utilized to assess MMP-13 activity in DPCs cultured in supplemented medium, mineralizing medium and SAHA-augmented mineralizing medium. The selected times for analysis (48 h, 14 d) were similar to microarray gene expression data, however, 48 h samples were more discriminative than 24 h, at which there no increase in enzyme activity (data not shown); a finding supported by previous experimentation (Lei et al., 2013). MMP-13 activity significantly increased in the extracts of DPC cell pellets at both 48 h and 14 days, both in the presence of mineralizing medium (48 h, p=0.009; 14 d p<0.0001) and mineralizing medium + SAHA (48 h, p<0.0001; 14 d p<0.0001) compared with a supplemented control (Fig. 4C/D), confirming that MMP-13

18

activity as well as protein expression was increased in mineralizing cultures. When comparing only the groups cultured in mineralizing conditions, the addition of SAHA significantly increased activity over HDACi-free cultures at 48 h (p=0.042) and 14 days (p=0.041), supporting the transcriptomic and ELISA data. The addition of a specific MMP-13i reduced enzyme activity compared with inhibitor-free mineralizing cultures, but not significantly at 48 h (p=0.09) (Fig. 4C) and 14 days (p=0.131) (Fig. 4D). Notably, a significant reduction in MMP-13 activity was evident when a MMP-13i was added to the SAHA mineralizing cultures at both 48 h (p=0.048) and 14 days (p=0.001). Interestingly, the addition of a MMP-13i reduced the enzyme activity to levels below that of the mineralizing culture controls.

MMP-13 inhibition promotes mineralization in dental pulp cells in both the presence and absence of SAHA at concentrations not reducing cell growth or viability. As previous data demonstrated that 1 µM SAHA increased both mineralization and mineralization-associated transcript levels, we hypothesised that specific inhibition of MMP-13 would inhibit DPC mineralization. To investigate the mineralizing effect of MMP-13, a repeat of the previous 14 day SAHA mineralization experiment in the presence or absence of a selective MMP-13i was performed. The MMP-13i concentrations selected (1 and 2 µM) were chosen based both on the previous results of the enzyme activity assays and a cell growth assay which demonstrated that DPC growth was only significantly inhibited (reduced by 15%) at 24 h in the samples containing a combination of 1 µM SAHA and 2 µM MMP-13i (p=0.01), compared with HDACi-free mineralizing control cultures (Fig. 5A). Other groups containing SAHA alone or in combination with 1 µM MMP-13i demonstrated no significant effect on growth (p>0.128). At 5 days, the results differed with significant growth inhibition evident for all three HDACi-containing cultures, SAHA alone (p=0.005), SAHA + 1 µM MMP-13i (p=0.002) and SAHA + 2 µM MMP-13i (p=0.004) compared with mineralizing control cultures. Notably, in the absence of SAHA both 1 and 2 µM MMP-13i did not significantly inhibit DPC growth (p>0.974). DPC viability, assessed by Trypan blue exclusion, was not significantly affected by any of the concentrations of MMP-13i used in this study (results not shown). As

19

the MMP-13i was not shown to affect growth or viability, both concentrations were investigated in a mineralization assay in the presence and absence of 1 µM SAHA.

In both the presence and absence of SAHA, MMP-13 inhibition increased matrix mineralization dose-dependently (Fig. 5B), with significant increases in mineralization evident in the SAHA-free group with 2 µM MMP-13i (p=0.12) and in the SAHA group in combination with 1 and 2 µM MMP-13i (p=-0.016/p=0.001), respectively. As a dose-dependent MMP-13i-induced mineralization response in DPCs was observed with Alizarin red staining, further analysis of differentiation was assessed by analysis of gene expression for several mineralization-associated transcripts (Fig. 5Ci-v). The transcripts were selected based on the results of this studies validatory RT-PCR, with a focus on HDACi-induced genes demonstrated to have a role in the dental pulp mineralisation process; BMP-4 (Duncan et al., 2012), Adrenomedullin (Musson et al., 2010), Osteopontin (Duncan et al., 2013), MMP-9 (Wu et al., 2015) and IBSP (Gopinathan et al., 2013). At 24 h MMP-13 inhibition significantly increased IBSP (p=0.003) and MMP-9 (p=0.014) transcript levels, while at 5 days IBSP (p=0.035), ADM (p=0.036) and Osteopontin (p=0.011) levels were increased compared with the mineralizing medium control (Fig. 5Ci-v). Furthermore, combinations of SAHA and MMP-13i in culture also significantly increased expression of BMP-4 (p=0.041), IBSP (p=0.048), ADM (p=0.002), Osteopontin (p=0.015) and MMP-9 (p=0.014) at 24 h and BMP-4 (p=0.001), IBSP (p=0.002), ADM (p=0.013), Osteopontin (p=0.002) and MMP-9 (p=0.003) at 5 days compared with the mineralizing medium control.

MMP-13 specific inhibition suppresses SAHA-enhanced dental pulp cell migration. Wound healing in the damaged dental pulp involves the migration of progenitor cells to the site of injury (Yoshiba et al., 1996). HDACis, including SAHA, have previously been shown to increase migration in various cell types (Lin et al., 2012), while MMP-13 is known to regulate cell migration through its action on cell phenotype (Lei et al., 2013). Subsequently, we hypothesised that two low concentrations of HDACi (1, 3 µM) would stimulate migration of DPCs in a transwell migration assay and that inhibition of MMP-13 activity may reduce this effect. Using transwell migration and wound healing scratch assay, primary DPC migration

20

was investigated *in vitro* following 3 h SAHA treatment. The transwell assay demonstrated a significant increase in primary DPC migration of 24% and 38% in the presence of 1 µM (p=0.007) and 3 µM (p<0.001) SAHA, respectively, compared with the negative control (Fig. 6A). No significant increase in cell migration compared with the control was evident after the addition of 1 µM (p=0.157) or 2 µM (p=0.253) MMP-13i in the absence of SAHA. The combination of 2 µM MMP-13i and 1 µM SAHA significantly suppressed the SAHA-induced migration (p=0.013). These data indicate that MMP-13 expression may be partly responsible for the enhanced cell migratory effects demonstrated. These results were further corroborated by the wound healing 'scratch' assay in DPC monolayers (Fig. 6B), which demonstrated significantly enhanced DPC migration in the presence of 1 µM SAHA (p=0.049) compared with the control, while notably the addition of 2 µM MMP-13i (p=0.999) alone or in combination with 1 µM SAHA (p=0.945) had no significant effect on wound healing (Fig. 6C-D).

Discussion

Dental pulp tissue has the ability to repair by the migration of a progenitor cell population to the injury site and their differentiation into odontoblast-like cells by the defensive process of reparative dentinogenesis (Smith et al., 2008). Dentistry exploits these regenerative capabilities clinically using a range of restorative procedures, however, there is a need to improve the clinical success of these treatments and develop novel pulp regenerative tissue engineering strategies (Murray et al., 2007). Several *in vitro* studies have indicated that HDACis offer the potential to promote regenerative processes by increasing differentiation of dental pulp cell populations (Duncan et al., 2011; Duncan et al., 2012; Jin et al., 2013; Paino et al., 2014). In this study, we for the first time characterised epigenetically-modified gene expression events that occur in SAHA-treated DPCs, identifying up-regulated pathways and key mediators. Our novel data indicates that SAHA modulates pulpal MMP expression, specifically increasing the activity of MMP-13, which is partly responsible for modulating mineralization and DPC migratory events.

21

Previous DPC experimentation using different HDACi (VPA, TSA) demonstrated acceleration of matrix mineralization (Duncan et al., 2013; Jin et al., 2013; Paino et al., 2014) and in the present study, the initial hypothesis that SAHA did not induce significant anti-proliferative, apoptotic or necrotic effects, but could stimulate *in vitro* mineralization was confirmed. The importance of the HDACi-concentration on mineralization is also highlighted, with the observed dose-dependent increase consistent with previous studies utilising osteoblast (Cho et al., 2005), dental-papilla derived cell lines (Duncan et al., 2012; Kwon et al., 2012) and primary DPCs (Duncan et al., 2013). As HDACi-induced mineralization was accelerated over a relatively narrow range of low SAHA concentrations, it is critical that optimal concentration parameters are established for each individual HDACi. Supporting previous results using VPA and TSA (Duncan et al., 2012), SAHA induced mineralization (>2-fold increase) in cultures supplemented with 24 h SAHA, prior to HDACi-free culture for the remainder of the 14 day experiment. Notably, extension of the SAHA supplementation (14 days, changed every 3 days) inhibited mineralization deposition and highlighting the critical importance of HDACi-treatment duration. This finding could help explain the paradoxical findings that HDACis stimulate osteogenic mineralization *in vitro* (Sakata et al., 2004; Cho et al., 2005; Schroeder and Westendorf, 2005; De Boer et al., 2006), but long-term *in vivo* oral VPA administration in humans (Nissen-Meyer et al., 2007), or 3-4 week systemic administration in mice (McGee-Lawrence et al., 2011) results in overall bone loss. It was previously proposed that the bone loss was due to a reduction in immature osteoblast numbers *in vivo*, while *in vitro* mature osteoblast populations were resistant to the detrimental effects of HDACi (McGee-Lawrence and Westendorf, 2011), however, it was recently demonstrated in mice that reducing the frequency of *in vivo* SAHA administration (from daily to every 3 days) resulted in no animal weight loss or cell toxicity (Xu et al., 2013). Our results highlight that limiting the HDACi-exposure, as well as establishing optimal concentration levels, is critical to avoid possible the HDACi-induced mesenchymal stem cell toxicity referred to in previous studies (Xu et al., 2013).

Despite recent advances, the mechanisms driving dentine matrix mineralization and HDACi-induced promotion of pulp cell mineralization remain to be elucidated. This study clearly demonstrates

22

the SAHA induced differential expression of several novel genes in primary rat DPCs cultured under

mineralizing conditions at early (24 h) and later time points (14 d). Furthermore, the involvement of many

of the identified transcripts has not previously been identified in HDACi microarray studies (Tables 2-5).

The observed differences are likely to be attributable to the cell type (i.e. rat primary DPCs have not

previously been studied in this context), the mineralizing conditions and the relatively short duration of

SAHA exposure (24 h). Similarly to previous HDACi high-throughput array studies, genes were both

induced and suppressed by SAHA (LaBonte et al. 2009; Dudakovic et al., 2013), however, notably at 24

h more genes were suppressed, highlighting tissue-dependent differences in HDACi-induced effects. Only

a relatively small number (3.3%) of SAHA induced genes showed a significant >2.0-fold transcriptional

change at 24 h, which reduced to 0.15% at 14 days, demonstrating that 24 h SAHA-induced effects are

generally reversible and do not persist through to the mineralization stage (Fig. 2A). The labile nature of

histone tail acetylation has been shown in other recent microarray studies in non-mineralizing cultures

(Boudadi et al., 2013), but may also be a particular feature of the binding characteristics of the particular

HDACi (Lauffer et al., 2013). SAHA and other hydroxamate-containing HDACi have been described as

having short-residence times compared with other benzamide-containing inhibitors (Lauffer et al., 2013).

By logical extrapolation, it is therefore to be expected that various HDACis are likely to differentially

affect the expression of different genes due to variations in potencies, binding characteristics and

specificities (Schroeder et al., 2007; Khan et al., 2008; Lauffer et al., 2013. However, SAHA was selected

for this study due to its FDA clinical approval (SAHA=voronostat, Zolinza™), frequent experimental use

and positive mineralization-inducing action compared with other HDACis (Kwon et al., 2012). Indeed,

comparison of our data with the nearest equivalent set of osteogenic gene array data (Schroeder et al.,

2007), shows a similar pattern of expression, despite differences in cell type (preosteoblasts vs primary

DPCs), treatment time (18 h vs 24 hr) and HDACi (TSA, MS-275 vs SAHA). Notably, several genes

identified as potentially responsible for osteoblast maturation (Schroeder et al., 2007) were also

upregulated in the current study, such as the apical membrane phosphoprotein, Slc9a3r1 (Fig. 2C) and

glutathione S-transferase alpha 4 (Table 2), while other common cell cycle genes were down-regulated

including Cyclin A1, Cyclin B2 and Polo-like kinase 1 and 4 (Table 3). Indeed, if a range of HDACi-specific gene array studies are compared there is significant overlap in the differentially expressed genes identified (see final column in Tables 2-5). The SAHA induced down-regulation of cell cycle associated-genes (Cyclin A1, B2) was supported by reduced DPC growth at 5 days (Fig. 5A), while, DPC mineralization was increased concomitantly (Figs 1C & 5B); supporting a theory that SAHA reduced the proliferation of DPCs, while promoting cell differentiation.

Gene expression microarray, pathway and qRT-PCR analyses identified the up-regulation of several members of the MMP family (notably MMP-9, MMP-13) (Fig. 2D) as well as other key genes responsible for degradation of extracellular matrix, such as Ctsl-1 and Plat and other tissue proteases, including ADAMTS 9 and 5. It has recently been noted *in vivo* that tissue inhibitor of matrix metalloproteinase 1, (TIMP-1), MMP-3 and MMP-13 expression can be upregulated in DPCs *in vivo* 3 days after cavity preparation in rodent teeth and the authors highlighted a potential role in pulp repair (Yoshioka et al., 2013). In our study, although MMP-3 expression was not increased by HDACi, TIMP-1 gene expression was increased at 24h by SAHA (1.6-fold at 24 h). Furthermore, our pathway and gene expression analysis (both microarray and RT-PCR) indicated that 1 µM SAHA up-regulated the expression of MMP-13 and a range of other proteolytic signalling molecules (Fig. 2D). The expression of a range of MMPs has previously been demonstrated to be induced by HDACi in various cell types (Mayo et al, 2003; Schroeder et al., 2007 Lin et al., 2012), but not specifically linked to modulation of the mineralization process. In addition, it was previously reported that HDAC-4 repressed MMP-13 gene expression in bone (Shimizu et al., 2010) and in a subsequent studies, that parathyroid activation of MMP-13 transcription required HAT activity (Lee and Partridge, 2010) and was negatively regulated by SIRT-1 (Fei et al., 2015), highlighting an interaction between HDACs/HAT, mineralization and MMP-13. While it is accepted that other MMP members may have important roles (e.g. MMP-9, MMP-2) in mineralization, previous findings prompted us to examine the interaction between SAHA and MMP-13 in order to characterise an as yet unidentified role for MMP-13 in pulp matrix mineralization. We show here that MMP-13 protein expression is increased in mineralizing DPCs and further increased in the presence

24

of SAHA. Furthermore, after the addition of a selective MMP-13 antagonist, there was increased expression of several mineralization-associated genes (BMP-4, IBSP), as well as MMP-13 enzyme activity at early and late time-points. This highlights a central role for MMP-13 in modulating mineralization processes in the pulp supporting a previous proposal (Suri et al., 2008).

A possible explanation for this less straightforward observation is that MMP-13 inhibition increased matrix calcification in mineralizing cultures in the presence or absence of SAHA. MMP-13 expression has been linked to the promotion of regenerative responses (Toriseva et al., 2007) and differentiation (Lei et al., 2013) in certain cell types, however, it has been reported in other tissues that MMP-13 inhibition can stimulate increased differentiation (Wu et al., 2002b; Nishimura et al., 2012). Within this and other studies (Winchester et al., 1999; Suri et al., 2008), MMP-13 protein expression was increased in mineralizing cultures and here we showed a further increase in the presence of SAHA. Logically, it might have been expected that inhibiting a collagenase, such as MMP-13, would reduce matrix mineralization, however, paradoxically mineralization was increased with selective MMP-13 inhibition. It can be speculated that this may result from a feedback mechanism in which MMP-13 expression facilitates an ordered deposition of mineral, thus preventing the formation of excessive or low quality mineral (Staines et al., 2014). This theory is supported by the results of MMP-13 knockout mice experimentation in which ossification is delayed and collagen accumulates in growth plate regions (Yamagiwa et al., 1999; Inada et al., 2004), as well as an impaired bone healing and remodelling after fracture (Behonick et al., 2007). Additionally, it is likely that tissue proteases, including MMP-13, have broader reparative roles in the pulp cleaving bioactive growth factors or releasing dentine matrix proteins from the matrix to stimulate cell migration and promote differentiation (Ortega et al., 2003) (Fig. 7). In this study, the promotion of mineralization processes by HDAC and MMP-13 inhibitors is supported by RT-PCR, as mineralization-associated gene expression was enhanced at two time-points, including a further increase in MMP-9 expression, a transcript identified by gene expression analysis as being significantly upregulated by SAHA alone at 24 h. Although not specifically investigated in this study, it has been previously demonstrated by others that MMPs and their inhibitors may form part of an intricate

25

network of support, feedback and synergy; regulating the activity of other MMPs (Ortega et al., 2003). Indeed, MMP-9 and MMP-13 have been previously reported to act synergistically in their effects on bone remodelling and development (Engsig et al., 2000) and may act similarly within dental pulp tissue.

Dental pulp healing after injury has classically been described as a two-stage process (Schröder, 1985), initially involving vascular and defence cell proliferation, migration and adhesion aiming to eliminate the injurious microbial irritant. Thereafter, wound repair proceeds with proliferation, migration and adhesion of various cells including progenitor or stem cells, which will differentiate under the influence of various bioactive molecules to odontoblast-like cells to produce reparative tertiary dentine (Smith et al., 1995; Smith et al., 2002; Smith et al., 2008). Cancer studies investigating neoplastic cell migration have demonstrated that even at low concentrations, a range of HDACi can increase cell migration; this finding was attributed to the epigenetic activation of gene transcription, tumour-progressive genes and a change in cell phenotype in HDACi treated cells (Lin et al., 2012). Mechanistically, HDACi-enhanced cell migration has been shown to activate a range of transcripts including chemokine receptors, integrins, glycodelin, and the serine protease urokinase plasminogen activator (UPA) (Lin et al., 2005; Mori et al., 2005; Uchida et al., 2007; Pulukuri et al., 2007). Within the current study, at 24 h UPA was not significantly increased in expression, however, other studies have reported that MMPs released from tumour cells are crucial not only for tissue degradation *in vivo*, but also cell migration observed *in vitro* (Liotta et al., 1980; Laurenzana et al., 2013). Interestingly, it appears that in regenerating tissues MMP-13 activity is central to cell migration, playing an important role in skeletal muscle repair and myoblast migration (Lei et al., 2013), and cutaneous wound healing (Wu et al., 2002a; Hattori et al., 2009). In addition, pathological expression of MMP-13 has been attributed to increased growth and metastatic invasion capacity of squamous cell carcinoma *in vivo* (Ala-aho et al., 2004). However, HDAC inhibition demonstrates conflicting results with regard to cell migration with some studies reporting a significant increase in cell migration *in vitro* (Uchida et al., 2007; Spallotta et al., 2013), while others reporting the opposite effect (Laurenzana et al., 2013). The rationale for these differences could be cell type-dependent, but this may also be a concentration effect with higher doses of

26

HDACis generally being shown to reduce cell migration (Uchida et al., 2007). Within the present study, low concentrations of SAHA dose-dependently increased DPC migration, in both cell monolayer and in transwell migration assays, an effect which was blocked by a selective MMP-13 inhibitor. Potentially, the HDACi-induced increase in MMP-13 expression could further enhance migration *in vivo* by promoting cleavage of growth factors or release of matrix proteins and increase chemotaxis (Ortega et al., 2003; Paiva and Granjeiro, 2014). DPC migration effects have translational relevance, as SAHA could be applied to the exposed pulp surface during vital pulp treatment; this could induce MMP-13 expression, potentially promoting the migration of dental progenitor cells from the centre of the pulp to the wound surface for differentiation into odontoblast-like cells during reparative dentinogenesis.

HDACi have been shown to promote mineralization responses by the induction of a range of genes in osteoblast cultures (Schroeder et al., 2007). Here we report that histone deacetylation promotes DPC mineralization and induces MMP-13 expression and activity at both early and late time-points, while MMP-13 also mediates a SAHA-induced increase in DPC migration. From a translational perspective the promotion of tissue-repair processes was evident after a 24 h dose of topical SAHA, highlighting the potential benefit of topical HDACi application to damaged dental pulps during regenerative vital pulp treatment.

27

References

Ala-aho R, Ahonen M, George S J, Heikkilä JR, Grénman Kallajoki M, Kähäri VM. 2004. Targeted inhibition of human collagenase-3 (MMP-13) expression inhibits squamous cell carcinoma growth in vivo. Oncogene 23:5111-5123.

Behonick DJ, Xing Z, Lieu S, Buckley J M, Lotz JC, Marcucio RS, Wern Z, Miclau T, Colnot C. 2007. Role of matrix metalloproteinase 13 in both endochondral and intramembranous ossification during skeletal regeneration. PLoS One 7:e1150.

Bolden JE, Peart MJ, Johnstone RW. 2006. Anticancer activities of histone deacetylase inhibitors. Nat Rev Drug Discov 5:769-784.

Boudadi E, Stower H, Halsall JA, Rutledge CE, Leeb M, Wutz A, O'Neill LP, Nightingale KP, Turner BM. 2013. The histone deacetylase inhibitor sodium valproate causes limited transcriptional change in mouse embryonic stem cells but selectively overrides Polycomb-mediated Hoxb silencing. Epigenetics Chromatin 6, 11.

Borzí RM, Olivotto E, Pagani S, Vitellozzi R, Neri S, Battistelli M, Falcieri E, Facchini A, Flamigni F, Penzo M, Platano D, Santi S, Facchini A, Marcu KB. 2010. Matrix metalloproteinase 13 loss associated with impaired extracellular matrix remodeling disrupts chondrocyte differentiation by concerted effects on multiple regulatory factors. Arthritis Rheum 62:2370–2381.

Bracker TU, Sommer A, Fichtner I, Faus H, Haendler B, Holger H-S. 2009. Efficacy of MS-275, a selective inhibitor of class I histone deacetylases, in human colon cancer models. Int J Oncol 35, 909-920.

28

Bradley EW, McGee-Lawrence ME, Westendorf JJ .2011. HDAC-mediated control of endochondral and intramembranous ossification. Crit Rev Eukaryot Gene Expr 21:101–113.

Charadram N, Farahani RM, Harty D, Rathsam C, Swain MV, Hunter N. 2012. Regulation of reactionary dentin formation by odontoblasts in response to polymicrobial invasion of dentin matrix. Bone 50:265–275.

Cho HH, Park HT, Kim YM, Bae YC, Suh KT, Jung JP. 2005. Induction of osteogenic differentiation of human mesenchymal stem cells by histone deacetylease inhibitors. J Cell Biochem 96, 533-542.

De Boer J, Licht R, Bongers M, van der Klundert T, Arend R, van Blitterswijk C. .2006. Inhibition of histone acetylation as a tool in bone tissue engineering. Tissue Eng 12:2927-2937.

de Groh ED, Swanhart LM, Cosentino CC, Jackson RL, Dai W, Kitchens CA, Day BW, Smithgall TE, Hukriede NA. 2010. Inhibition of histone deacetylase expands the renal progenitor cell population. J Am Soc Nephrol 21:794-802.

Dudakovic A, Evans JM, Ying L, Middha S, McGee-Lawrence ME, van Wijnen AJ, Westendorf JJ. 2013. Histone Deacetylase Inhibition Promotes Osteoblast Maturation by Altering the Histone H4 Epigenome and Reduces Akt Phosphorylation. J Biol. Chem. 288:28783–28791.

Duncan HF, Smith AJ, Fleming GJ, Cooper PR. 2011. HDACi: cellular effects, opportunities for restorative dentistry. J Dent Res 90:1377-1388.

Duncan HF, Smith AJ, Fleming GJ, Cooper PR. 2012. Histone deacetylase inhibitors induced differentiation and accelerated mineralization of pulp-derived cells. J Endod 38:339-345.

Duncan HF, Smith AJ, Fleming GJ, Cooper PR. 2013. Histone deacetylase inhibitors epigenetically promote reparative events in primary dental pulp cells. Exp Cell Res 319:1534-1543.

Engsig MT, Chen QJ, Vu TH, Pedersen AC, Therkidsen B, Lund LR, Henriksen K, Lenhard, T, Foged NT, Werb Z, Delaissé JM. 2000. Matrix metalloproteinase 9 and vascular endothelial growth factor are essential for osteoclast recruitment into developing long bones. J Cell Biol 151:879-889.

Fazi B, Melino S, De Rubeis S, Bagni C, Paci M, Piacentini M, Di Sano F. 2009. Acetylation of RTN-1C regulates the induction of ER stress by the inhibition of HDAC activity in neuroectodermal tumors. Oncogene 28:3814–3824.

Fei Y, Shimizu E, McBurney MW, Partridge NC. 2015. Sirtuin 1 is a Negative Regulator of Parathyroid Hormone Stimulation of Matrix Metalloproteinase 13 Expression in Osteoblastic Cells. J Biol Chem 290:8373-8382.

Fischer C, Drexler HG, Reinhardt J, Zaborski M, Quentmeier H. 2007. Epigenetic regulation of brain expressed X-linked-2, a marker for acute myeloid leukemia with mixed lineage leukemia rearrangements. Leukemia 21:374–377.

Foltz G, Ryu G-Y, Yoon J-G, Nelson T, Fahey J, Frakes A, Lee H, Field L, Zander K, Sibenaller Z, Ryken TC, Vibhakar R, Hood L, Madan A. 2006. Genome-Wide Analysis of Epigenetic Silencing Identifies BEX1 and BEX2 as Candidate Tumor Suppressor Genes in Malignant Glioma. Cancer Res 66:6665-6674.

30

Gopinathan G, Kolokythas A, Luan X, Diekwisch TG. 2013. Epigenetic marks define the lineage and differentiation potential of two distinct neural crest-derived intermediate odontogenic progenitor populations. Stem Cells Dev 22:1763-1778.

Grant S, Easley C, Kirkpatrick P. 2007. Vorinostat. Nat Rev Drug Discov 6:21-22.

Gregoretti IV, Lee YM, Goodson HV. 2004. Molecular evolution of the histone deacetylase family: functional implications of phylogenetic analysis. J Mol Biol 338:17-31.

Gregory CA, Gunn WG, Peister A, Prockop DJ. 2004. An Alizarin red-based assay of mineralization by adherent cells in culture: comparison with cetylpyridinium chloride extraction. Anal Biochem 329:77-84.

Haigis M C, Guarente LP. 2006. Mammalian sirtuins emerging roles in physiology, aging, and calorie restriction. Genes Dev 20:2913-2921.

Hannas AR, Pereira JC, Granjeiro JM, Tjäderhane L. 2007. The role of matrix metalloproteinases in the oral environment. Acta Odontol Scand 65:1-13.

Hattori N, Mochizuki S, Kishi K, Nakajima T, Takaishi H, D'Armiento J, Okada Y. 2009. MMP-13 plays a role in keratinocyte migration, angiogenesis, and contraction in mouse skin wound healing. Am J Pathol 175:533-546.

Inada M, Wang Y, Byrne MH, Rahman MU, Miyaura C, López-Otín C, Krane SM. 2004. Critical roles for collagenase-3 (Mmp13) in development of growth plate cartilage and in endochondral ossification. Proc Natl Acad Sci USA 101:17192–17197.

31

Jin H, Park JY, Choi H, Choung PH. 2013. HDAC inhibitor trichostatin A promotes proliferation and odontoblast differentiation of human dental pulp stem cells. Tissue Eng Part A 19:613-624.

Kelder T, van Iersel MP, Hanspers K, Kutmon M, Conklin BR, Evelo CT, Pico AR. 2012. WikiPathways: building research communities on biological pathways. Nucleic Acids Res 40:D1301-1307.

Khan N, Jeffers M, Kumar S, Hackett C, Boldog F, Khramtsov N, Qian X, Mills E, Berghs SC, Carey N, Finn PW, Collins LS, Tumber A, Ritchie JW, Jensen PB, Lichenstein HS, Sehested M. 2008. Determination of the class and isoform selectivity of small-molecule histone deacetylase inhibitors. Biochem J 409:581-589.

Klinz FJ, Korkmaz Y, Bloch W, Raab WH, Addicks K. 2012. Histone deacetylases 2 and 9 are coexpressed and nuclear localized in human molar odontoblasts in vivo. Histochem Cell Biol 137:697-702.

Koutsounas I, Giaginis C, Patsouris E, Theocharis S. 2013. Current evidence for histone deacetylase inhibitors in pancreatic cancer. World J Gastroenterol 19:813-828.

Krane SM, Inada M. 2003. Matrix metalloproteinases and bone. Bone 43:7-18.

Kwon A, Park HJ, Baek K, Lee HL, Park JC, Woo KM, Ryoo HM, Baek JH. 2012. Suberoylanilide hydroxamic acid enhances odontoblast differentiation. J Dent Res 91:506-512.

LaBonte MJ, Wilson PM, Fazzone W, Groshen S, Lenz H-J, Ladner RD. 2009. DNA microarray profiling of genes differentially regulated by the histone deacetylase inhibitors vorinostat and LBH589 in colon cancer cell lines. BMC Medical Genomics 2:67.

32

Lauffer BE, Mintzer R, Fong R, Mukund S, Tam C, Zilberleyb I, Flicke B, Ritscher A, Fedorowicz G, Vallero R, Ortwine DF, Gunzer J, Modrusan Z, Neumann L, Koth CM, Lupardus, PJ, Kaminker JS, Heise CE, Steiner P. 2013, Histone Deacetylase (HDAC) Inhibitor Kinetic Rate Constants Correlate with Cellular Histone Acetylation but Not Transcription and Cell Viability. J Biol Chem. 288:26926-26943.

Laurenzana A, Balliu M, Cellai C, Romanelli MN, Paoletti F. 2013. Effectiveness of the histone deacetylase inhibitor (S)-2 against LNCaP and PC3 human prostate cancer cells. PLoS One 8:e58267.

Lee M, Partridge NC. 2010. Parathyroid hormone activation of matrix metalloproteinase-13 transcription requires the histone acetyltransferase activity of p300 and PCAF and p300-dependent acetylation of PCAF. J Biol Chem 285:38014-38022.

Lee HS, Park MH, Yang SJ, Jung HY, Byun SS, Lee DS, Yoo HS, Yeom Y I, Seo SB. 2004. Gene Expression Analysis in Human Gastric Cancer Cell Line Treated with Trichostatin A and S-Adenosyl-L-homocysteine Using cDNA Microarray. Biol Pharm Bull 27:1497-1503.

Lei H, Leong D, Smith LR, Barton ER. 2013. Matrix metalloproteinase 13 is a new contributor to skeletal muscle regeneration and critical for myoblast migration. Am J Physiol Cell Physiol 305:C529–C538.

Li CJ, Li RW. 2008. Butyrate Induced cell cycle arrest in bovine cells through targeting gene expression relevant to DNA replication apparatus. Gene Regul Syst Biol 2:113-123.

Lin KT, Yeh SH, Chen DS, Chen PJ, Jou YS. 2005. Epigenetic activation of alpha4, beta2 and beta6 integrins involved in cell migration in trichostatin A-treated Hep3B cells. J Biomed Sci 12:803–813.

33

Lin KT, Wang YW, Chen CT, Ho CM, Su WH, Jou YS. 2012. HDAC inhibitors augmented cell migration and metastasis through induction of PKCs leading to identification of low toxicity modalities for combination cancer therapy. Clin Cancer Res 18:4691–4701.

Liotta LA, Tryggvason K, Garbisa S, Hart I, Foltz CM, Shafie S. 1980. Metastatic potential correlates with enzymatic degradation of basement membrane collagen. Nature 284:67–68.

Liu Y, Hea G, Wanga Y, Guana X, Pangb X, Zhanga B. 2013. MCM-2 is a therapeutic target of Trichostatin A in colon cancer cells. Toxicol Lett 221:23-30.

McGee-Lawrence ME, McCleary-Wheeler AL, Secreto FJ, Razidlo DF, Zhang M, Stensgard B A, Li X, Stein GS, Lian JB, Westendorf JJ. 2011. Suberoylanilide hydroxamic acid (SAHA; vorinostat) causes bone loss by inhibiting immature osteoblasts. Bone 48:1117-1126.

McGee-Lawrence ME, Westendorf JJ.2011. Histone deacetylases in skeletal development and bone mass maintenance. Gene 474:1-11.

Mahmud N, Petro B, Baluchamy S, Li X, Taioli S, Lavelle D, Quigley JG, Suphangul M, Araki H. 2014. Differential effects of epigenetic modifiers on the expansion and maintenance of human cord blood stem/progenitor cells. Biol Blood Marrow Transplant 20:480-489.

Majumdar G, Adris P, Bhargava N, Chen H, Raghow R. 2012. Pan-histone deacetylase inhibitors regulate signaling pathways involved in proliferative and pro-inflammatory mechanisms in H9c2 cells. BMC Genomics 13:709.

34

Marks PA, Dokmanovic M. 2005. Histone deacetylase inhibitors: discovery and development as anticancer agents. Exp Opin Investig Drugs 14:1497-1511.

Marks PA, Xu WS. 2009. Histone deacetylase inhibitors: potential in cancer therapy. J Cell Biochem. 107:600-608.

Marks PA. 2010. Histone deacetylase inhibitors: a chemical genetics approach to understanding cellular functions. Biochim Biophys Acta: Gene Regulatory Mechanisms 1799:717-725.

Mayo MW, Denlinger CE, Broad RM, Yeung F, Reilly ET, Shi Y, Jones D. 2003. Ineffectiveness of Histone Deacetylase Inhibitors to Induce Apoptosis Involves the Transcriptional Activation of NF-kB through the Akt Pathway. J Biol Chem 278:18980-18989.

Milli A, Cecconi D, Campostrini N, Timperio AM, Zolla L, Righetti SC, Zunino F, Perego P, Benedetti V, Gatti L, Odreman F, Vindigni A, Righetti PG. 2008. A proteomic approach for evaluating the cell response to a novel histone deacetylase inhibitor in colon cancer cells. Biochim Biophys Acta 1784:1702-1710.

Moore PS, Barbi S, Donadelli M, Costanzo C, Bassi C, Palmieri M, Scarpa A. 2004. Gene expression profiling after treatment with the histone deacetylase inhibitor trichostatin A reveals altered expression of both pro- and anti-apoptotic genes in pancreatic adenocarcinoma cells. Biochim Biophys Acta 1693:167-176.

Mori T, Kim J, Yamano T, Takeuchi H, Huang S, Umetani N, Koyanagi K, Hoon DS. 2005. Epigenetic up-regulation of C-C chemokine receptor 7 and C-X-C chemokine receptor 4 expression in melanoma cells. Cancer Res 65:1800-1807.

35

Murphy CJ, Campbell S, Araki-Sasaki K, Marfurt CF. 1998. Effects of norepinephrine on proliferation, migration and adhesion of SV-40 transformed human cornea epithelial cells. Cornea 17:529-536.

Murray PE, Garcia-Godoy F, Hargreaves KM. 2007. Regenerative endodontics: a review of current status and a call for action. J Endod 33:377-390.

Musson DS, McLachlan JL, Sloan AJ, Smith AJ, Cooper PR. 2010. Adrenomedullin is expressed during rodent dental tissue development and promotes cell growth and mineralization. Biol Cell 102:145-157.

Milutinovic S, D'Alessio AC, Detich N, Szyf M. 2007. Valproate induces widespread epigenetic reprogramming which involves demethylation of specific genes. Carcinogenesis 28:560–571.

Nagase H, Woessner Jr JF. 1999. Matrix metalloproteinases. J Chem Biol 274:21491–21494.

Nguyen-Tran DH, Hait NC, Sperber H, Qi J, Fischer K, Ieronimakis N, Pantoja M, Hays A, Allegood J, Reyes M, Spiegel S, Ruohola-Baker H. 2014. Molecular mechanism of sphingosine-1-phosphate action in Duchenne muscular dystrophy. Dis Model Mech 7:41-54.

Nishimura R, Wakabayashi M, Hata K, Matsubara T, Honma S, Wakisaka S, Kiyonari H, Shioi G, Yamaguchi A, Tsumaki N, Akiyama H, Yoneda T. 2012. Osterix regulates calcification and degradation of chondrogenic matrices through matrix metalloproteinase 13 (MMP13) expression in association with transcription factor Runx2 during endochondral ossification. J Biol Chem 287:33179–33190.

Nissen-Meyer LS, Svalheim S, Taubøll E, Reppe S, Lekva T, Solberg LB, Melhus G, Reinholt F P, Gjerstad L, Jemtland R. 2007. Levetiracetam, phenytoin and valproate act differently on rat bone mass, structure and metabolism. Epilepsia 48:1850-1860.

Noh JH, Song JH, Eun JW, Kim JK, Jung KH, Bae HJ, Xie HJ, Ryu JC, Ahn YM, Wee SJ, Park WS, Lee JY, Nam SW. 2009. Systemic cell-cycle suppression by Apicidin, a histone deacetylase inhibitor, in MDA-MB-435. Int J Mol Med 24:205-226.

Ooi L, Belyaev ND, Miyake K, Wood IC, Buckley NJ. 2006. BRG1 Chromatin remodeling activity Is required for efficient chromatin binding by repressor element 1-silencing transcription factor (REST) and facilitates REST-mediated repression. J Biol Chem 281:38974-38980.

Ortega N, Behonick D, Stickens D, Werb Z. 2003. How proteases regulate bone morphogenesis. Ann NY Acad Sci 995:109-116.

Paino F, La Noce M, Tirino V, Naddeo P, Desiderio V, Pirozzi G, De Rosa A, Laino L, Altucci, Papaccio G. 2014. Histone deacetylase inhibition with valproic acid downregulates osteocalcin gene expression in human dental pulp stem cells and osteoblasts: evidence for HDAC2 involvement. Stem Cells 32:279-289.

Paiva KB, Granjeiro JM. 2014. Bone tissue remodeling and development: focus on matrix metalloproteinase functions. Arch Biochem Biophys 561:74-87.

Palosaari H, Pennington CJ, Larmas M, Edwards DR, Tjäderhane L, Salo T. 2003. Expression profile of matrix metalloproteinases (MMPs) and tissue inhibitors of MMPs in mature human odontoblasts and pulp tissue. Eur J Oral Sci 111:117-127.

37

Patel M, Smith AJ, Sloan A, Smith G, Cooper PR. 2009. Phenotype and behaviour of dental pulp cells during expansion culture. Arch Oral Biol 54:898-908.

Poulaki V, Mitsiades CS, Kotoula V, Negri J, McMullan C, Miller JW, Marks P A, Mitsiades N. 2009. Molecular Sequelae of Histone Deacetylase Inhibition in Human Retinoblastoma Cell Lines: Clinical Implications. Invest Ophthalmol Vis Sci 50:4072–4079.

Pulukuri SM, Gorantla B, Rao JS. 2007. Inhibition of histone deacetylase activity promotes invasion of human cancer cells through activation of urokinase plasminogen activator. J Biol Chem 282:35594–35603.

Pryzbylkowski P, Oluwakemi O, Keen JC. 2008. Trichostatin A and 5 Aza-20 deoxycytidine decrease estrogen receptor mRNA stability in ER positive MCF7 cells through modulation of HuR. Breast Cancer Res Treat 111:15-25.

Ravanti L, Hakkinen L, Larjava H, Saarialho-Kere U, Foschi M, Han J, Kähäri VM. 1999. Transforming growth factor-beta induces collagenase-3 expression by human gingival fibroblasts via p38 mitogen-activated protein kinase. J Chem Biol 274:37292–37300.

Salomonis N, Nelson B, Vranizan K, Pico AR, Hanspers K, Kuchinsky A, Ta L, Mercola M, Conklin BR. 2009. Alternative Splicing in the Differentiation of Human Embryonic Stem Cells into Cardiac Precursors. PLoS Comput Biol. 5:e1000553.

Sakata R, Minami S, Sowa Y, Yoshida M, Tamaki T. 2004. Trichostatin A activates the osteopontin gene promoter through AP1 site. Biochem Biophys Res Commun 315:959-963.

Schröder U. 1985. Effects of calcium hydroxide-containing pulp-capping agents on pulp cell migration, proliferation, and differentiation. J Dent Res 64:541-548.

Schroeder TM, Westendorf JJ. 2005. Histone deacetylase inhibitors promote osteoblast maturation. J Bone Miner Res 20:2254-2263.

Schroeder TM, Nair AK, Staggs R, Lamblin AF, Westendorf JJ. 2007. Gene profile analysis of osteoblast genes differentially regulated by histone deacetylase inhibitors. BMC Genomics 8:362.

Shimizu E, Selvamurugan N, Westendorf JJ, Olson EN, Partridge NC. 2010. HDAC4 represses matrix metalloproteinase-13 transcription in osteoblastic cells, and parathyroid hormone controls this repression. J Biol Chem 285:9616-9626.

Shuttleworth SJ, Bailey SG, Townsend PA. 2010. Histone deacetylase inhibitors: new promise in the treatment of immune and inflammatory diseases. Curr Drug Targets 11:1430-1438.

Smith AJ, Cassidy N, Perry H, Bègue-Kirn C, Ruch JV, Lesot H. 1995. Reactionary dentinogenesis. Int J Dev Biol 39:273–280.

Smith AJ, Murray PE, Lumley PE. 2002. Preserving the vital pulp in operative dentistry: 1. A biological approach. Dent Update 29:64–69.

Smith AJ, Lumley PE, Tomson PL, Cooper PR. 2008. Dental regeneration and materials: a partnership. Clin Oral Investig 12:103–108.

39

Smith JG, Smith AJ, Shelton RM, Cooper PR. 2012. Recruitment of dental pulp cells by dentine and pulp extracellular matrix components. Exp Cell Res 318:2397-2406.

Spallotta F, Cencioni C, Straino S, Sbardella G, Castellano S, Capogrossi MC, Martelli F, Gaetano C. 2013. Enhancement of lysine acetylation accelerates wound repair. Commun Integr Biol 6:e25466.

Staines KA, Zhu D, Farquharson C, MacRae VE. 2014. Identification of novel regulators of osteoblast matrix mineralization by time series transcriptional profiling. J Bone Miner Metab 32:240-251.

Sulkala M, Pääkkönen V, Larmas M, Salo T, Tjäderhane L. 2004. Matrix metalloproteinase-13 (MMP-13, Collagenase-3) is highly expressed in human tooth pulp. Connect Tissue Res 45:231–237.

Suri L, Damoulis PD, Le T, Gagari E. 2008. Expression of MMP-13 (collagenase-3) in long-term cultures of human dental pulp cells. Arch Oral Biol 53:791-799.

Suzuki H, Gabrielson E, Chen W, Anbazhagan R, van Engeland M, Weijenberg MP, Herman JG, Baylin SE. 2002. A genomic screen for genes upregulated by demethylation and histone deacetylase inhibition in human colorectal cancer. Nature Genetics 31:141-149.

Tomson PL, Grover LM, Lumley PJ, Sloan AJ, Smith AJ, Cooper PR. 2007. Dissolution of bio-active dentine matrix components by mineral trioxide aggregate. J Dent 35:636-642.

Toriseva MJ, Ala-aho R, Karvinen J, Baker AH, Marjomäki VS, Heino J, Kähäri VM. 2007. Collagenase-3 (MMP-13) enhances remodeling of three-dimensional collagen and promotes survival of human skin fibroblasts. J Invest Dermatol 127:49–59.

Uchida H, Maruyama T, Ono M, Ohta K, Kajitani T, Masuda H, Nagashima T, Arase T, Asada H, Yoshimura Y. 2007. Histone deacetylase inhibitors stimulate cell migration in human endometrial adenocarcinoma cells through up-regulation of glycodelin. Endocrinology 148:896-902.

van Iersel MP, Kelder T, Pico AR, Hanspers K, Coort S, Conklin BR, Evelo C. 2008. Presenting and exploring biological pathways with PathVisio. BMC Bioinformatics 9:399.

Verdin E, Dequiedt F, Kasler HG. 2003. Class II histone deacetylases: versatile regulators. Trends Genet 19:286-293.

Verma RP, Hansch C. 2007. Matrix metalloproteinases (MMPs): Chemical-biological functions and (Q)SARs. Bioorg Med Chem 15:2223–2268.

Villagra A, Cheng F, Wang HW, Suarez I, Glozak M, Maurin M, Nguyen D, Wright KL, Atadja PW, Bhalla K, Pinilla-Ibarz J, Seto E, Sotomayor EM. 2009. The histone deacetylase HDAC11 regulates the expression of interleukin 10 and immune tolerance. Nat Immunol 10:92-100.

Winchester SK, Bloch SR, Fiacco GJ, Partridge NC. 1999. Regulation of Expression of Collagenase-3 in Normal, Differentiating Rat Osteoblasts. J Cell Physiol 181:479–488.

Wu N, Opalenik S, Liu J, Jansen ED, Giro MG, Davidson JM. 2002a. Real-time visualization of MMP-13 promoter activity in transgenic mice. Matrix Biol 21:149–161.

Wu C W, Tchetina EW, Mwale F, Hasty K, Pidoux I, Reiner A., Chen J, Van Wart HE, Poole A R. 2002b. Proteolysis Involving Matrix Metalloproteinase 13 (Collagenase-3) is required for chondrocyte differentiation that is associated with matrix mineralization. J Bone Miner Res 17:639-651.

41

Wu L, Wang F, Donly KJ, Wan C, Luo D, Harris SE, MacDougall M, Chen S. 2015. Establishment of immortalized mouse Bmp2 knock-out dental papilla mesenchymal cells necessary for study of odontoblastic differentiation and odontogenesis. J Cell Physiol 230:2588-2595.

Xu S, De Veirman K, Evans H, Santini GC, Vande Broek I, Leleu X, De Becker A, Van Camp B, Croucher P, Vanderkerken K, Van Riet I. 2013. Effect of the HDAC inhibitor vorinostat on the osteogenic differentiation of mesenchymal stem cells in vitro and bone formation in vivo. Acta Pharmacol Sin 34:699-709.

Yamagiwa H, Tokunaga K, Hayami T, Hatano H, Uchida M, Endo N, Takahashi HE. 1999. Expression of metalloproteinase-13 (Collagenase-3) is induced during fracture healing in mice. Bone 25:197–203.

Yoshiba K, Yoshiba N, Nakamura H, Iwaku M, Ozawa H. 1996. Immunolocalization of fibronectin during reparative dentinogenesis in human teeth after pulp capping with calcium hydroxide. J Dent Res 75:1590-1597.

Yoshioka S, Takahashi S, Abe M, Michikami I, Imazato S, Wakisaka S, Hayashi M. 2013. Activation of the Wnt/β-catenin pathway and tissue inhibitor of metalloprotease 1 during tertiary dentinogenesis. J Biochem 153:43-50.

Zhang J, Zhu QL, Huang P, Yu Q, Wang ZH, Cooper PR, Smith AJ, He W. 2013. CpG ODN-induced matrix metalloproteinase-13 expression is mediated via activation of the ERK and NF-kB signalling pathways in odontoblast cells. Int Endod J 46:666–674.

42

Figure legends

Fig. 1. Short-term SAHA application did not significantly reduce primary DPC proliferation, viability and apoptosis at low concentration, while mineralization was promoted dose-dependently. (A) SAHA supplemented DPC cultures for 24 h at a range of concentrations and cell numbers were ascertained by Trypan blue exclusion. The addition of SAHA significantly reduced primary cell growth at 3 and 5 µM, but not 1 µM. (B) The same SAHA concentrations as in (A) were analysed after 24 h and 48 h by a live/dead staining fluorogenic assay to analyse DPC viability and necrosis. Short-term SAHA supplementation (24 h, 48 h) significantly reduced cell viability only at higher (5 µM) SAHA concentrations after 48 h. (C) SAHA concentrations (0.25 - 5 µM) supplemented the mineralizing medium for 24 h or 14 days at the initiation of the experiment. The mineral production for SAHA is based on quantification of Alizarin Red S stain extracted from each experimental well and corresponding cell counts. Short-duration SAHA (24 h) accelerated mineralization per cell in DPCs dose-dependently at 14 days, while prolonged SAHA exposure inhibits differentiation and prevents matrix calcification. (D) Effects of 1 µM SAHA on DPC apoptosis and viability in DPCs. FC images for control (no HDACi) (E) and 1 µM SAHA (F) after Annexin V-PI staining. Viable cells were observed in the left lower quadrant, early apoptotic cells in the right lower quadrant and late apoptotic cells in the right upper quadrant and charted as % total number of cells. A negative control (No SAHA) and a selected candidate concentration of 1 µM SAHA was investigated by FC at 24 h. All charted data are represented as mean ±SEM. For all experimentation, four independent experiments (n=4) were performed in triplicate for each HDACi concentrations. In the FC experimentation, 10,000 cell events were measured for each experimental/control group (n=4). Statistically significant differences (p<0.05) between the experimental and control are marked by an asterisk (*) or (**).

Fig 2. The effects of short-term low dose SAHA on relatively early and late stage gene expression under mineralizing conditions. (A) A time-course plot (1 day and 14 days) generated in GeneSpring GX12 showing all altered genes (normalised intensity values) in the SAHA-supplemented DPC cultures compared with HDACi-free control cultures. Red lines indicate up-regulated genes and blue indicates down-regulated transcripts in the 24 h data. (B) Number of genes demonstrating >2 fold change after addition of SAHA. Heat maps showing gene expression along with a list of selected mineralization-associated genes (C) and MMPs/TIMPs (D) expressed by DPCs at 24 h and 14 days in SAHA-supplemented media compared with HDACi-free control cultures. All gene expression array experiments based on four biologically independent experiments (n=4).

Fig 3. Confirmatory gene expression using quantitative real-time-PCR. To validate microarray results, representative transcripts were quantified by qRT-PCR in untreated and SAHA-treated DPCs. (A) Selected up-regulated genes and (B) down-regulated genes at 24 h and (C) up- and down-regulated genes at 14 days expressed as fold increase over control. Error bars represent mean ± SEM of 4 independent experiments carried out in triplicate. Students t-test was used to ascertain statistical significance of experimental compared with control samples.

Fig 4. The effects of SAHA on MMP-13 protein expression and enzyme activity. (A) Cell lysates from selected time points (1, 7, 14 and 21 days) were normalised using a Bradford dye-binding method and total MMP-13 protein levels quantified for each time point. MMP-13 production was analysed by ELISA. (B) A range of MMP-13i concentrations were added to samples of recombinant MMP-9, -13 and enzyme activity was measured fluorogenically for each inhibitor concentration. MMP-13 activity was blocked dose-dependently, but MMP-9 was not significantly altered. All experimental MMP-13i concentrations tested significantly decreased MMP-13 enzyme activity. (C/D) The effects of SAHA and a pharmacological MMP-13i on MMP-13 enzyme activity in mineralizing DPCs. DPCs were cultured in mineralizing medium ± SAHA/MMP-13i and compared with mineralizing and non-mineralizing control cultures at 48 h (C) and 14 days (D). MMP-13 activity (measured fluorogenically) increased in mineralizing culture and in the presence of SAHA at both experimental time-points. As the commercial FRET substrate was preferentially, but not exclusively cleaved by MMP-13, the selective MMP-13 inhibition was used to analyse the role of MMP-13. Selective MMP-13 inhibition significantly reduced enzyme activity in the SAHA cultures. Error bars represent SEM of three independent experiments carried out in triplicate. Significant difference p<0.05, denoted by asterix (*) between experimental group and normal medium control, symbol (^) between experimental group and mineralizing medium control and symbol (‡) between mineralizing medium + SAHA and mineralizing medium + SAHA + MMP-13i.

Fig 5. The effects of a selective MMP-13i on primary DPC proliferation, mineralization and gene expression. (A) A selective MMP-13i supplemented SAHA and HDACi-free cultures for 24 h and 5 days at two concentrations (1 and 2 μM). Viable cell numbers ascertained by Trypan blue exclusion and cell counting. (B), *In vitro* calcification of DPCs under mineralizing conditions in the presence and absence of 1 and 2 μM MMP-13i compared with SAHA supplemented and HDACi-free control groups. Alizarin red staining was used to demonstrate calcium deposits at 14 days and results presented as a fold increase in mineralization over the respective controls. (C) DPCs were cultured in mineralizing medium in the

44

presence or absence of 1 μM SAHA and 2 μM MMP-13i for 24 h and 5 days. mRNAs were isolated, reverse transcribed and amplified using real-time PCR with primers for (i) BMP-4, (ii) IBSP, (iii) Adrenomedullin, (iv) Osteopontin and (v) MMP-9 an compared to a supplemented mineralization control. The relative levels of mRNAs were normalized to β-actin and then expressed as fold stimulation over control. For all experiments, the error bars represent SEM of three independent experiments performed in triplicate. Asterix (*), $p<0.05$ and (**), $p<0.005$.

Fig 6. The effects of SAHA and MMP-13 activity on dental pulp cell (DPC) migration. (A) Vertical migration of DPCs measured by transwell migration assay at 37°C for 3 h. Positive control (supplemented medium and 10% FCS), 1 μM and 3 μM SAHA had a statistically significantly greater effect on cell migration compared with the negative control. MMP-13i (1 and 2 μM) and SAHA in combination with 2 μM MMP-13i was not significantly different compared with the negative control, indicating the MMP-13 may be partly responsible for the migratory effects of DPCs). (B) Quantitative data from (C/D) showing cell migration in response to HDACis. (B) Horizontal migration of DPCs by wound healing scratch assay. The effect roles of 1 μm SAHA on the migration and motility of rat DPCs quantified from 24 hour scratch assay. Cells were treated with 1 μM SAHA for 24 h and a scratch made in the confluent cell monolayer. Images were obtained at 0 (Ci-iv) and 24 h post wounding (Di-iv). Values are mean ± SEM for 3 independent experiments carried out in triplicate. Asterisks (*) show significant differences compared with control ($p<0.05$). Scale bars indicate 100 μm.

Fig 7. Overview schematic illustration highlighting the potential roles of MMP-13 is reparative dentinogenesis. (A) HDACi (SAHA) applied topically to exposed damaged pulp tissue, accelerates mineralization processes (and the expression of a range of mineralization-associated transcripts) and increases expression of MMP-13 in pulp cells. The expression of MMP-13 is central to the control of mineralization processes and the activation of a range of bioactive molecules by cleavage. These molecules could potentially promote angiogenesis, mineralization and cell migration. Increased MMP-13 expression has also been shown in inflamed dental DP cell lines (Zhang et al., 2013), which may have additional implications for dental pup healing. (B) Dental progenitor cells migrate from vasculature in central pulp under influence of bioactive molecules to injury site. Thereafter, the progenitor cells differentiate into odontoblast-like cells. MMP-13 may directly influence this recruitment process by increasing cell migration or by cleavage of matrix-bound dentin matrix proteins to increase chemotaxis and differentiation. Additionally MMP-13 (and other MMP collagenases) will breakdown extracellular

1
2
3
4
5
6
7
8
9
10
11
12
13
14
15
16
17
18
19
20
21
22
23
24
25
26
27
28
29
30
31
32
33
34
35
36
37
38
39
40
41
42
43
44
45
46
47
48
49
50
51
52
53
54
55
56
57
58
59
60

matrix further increasing migration and stimulating repair. *C,* Fossilised dentine matrix proteins leach into the pulp as a result of caries (Smith et al., 2008) or restorative materials (Schröder, 1995; Tomson et al., 2007) to promote reparative events. Growth factors released by MMP-cleavage (including MMP-13) further stimulate reparative response.

For Peer Review

46

Gene	Primer sequence (5' → 3')	Size bps	NCBI Accession number
β-Actin	(F)-AGCCATGTACGTAGCCATCC (R)-ACCCTCATAGATGGGCACAG	115	NM_031144
Disabled homolog 1 (Drosophila) Dab1	(F)- CCAGGTCAAGTCCACAGAGT (R)- TCAGGTTTTCGGGAGGGTAC	106	NM_153621
T-cell differentiation protein (Mal2)	(F)- CTACGATGGTTGTGAAGCCG (R)- ACTGTCGGTTTCCAAGGAGT	155	NM_198786
RAS guanyl releasing protein 3 (calcium and DAG-regulated) (Rasgrp3)	(F)- CCTCTTGGTTCTGGCCTGTA (R)- GTCCAGGTCTCGGTGTCTAG	148	NM_001108009
Ameloblastin (Ambn)	(F)-GAAAACCCGGCTCTCCTTTC (R)- ATTCAGGGGTGATCAGTGGG	157	NM_012900
Keratin 18 (Krt18)	(F)- CTGGGGCCACTACTTCAAGA (R)- GCGGAGTCCATGAATGTCAC	184	NM_053976
Eph receptor A3 (Epha3)	(F)- ATATGCTCCTCTCACTGCCC (R)- CGTGGGATGGGTAGGAGATC	185	NM_031564
Matrix metalloproteinase 13 (Mmp13)	(F)- AAGTGTGACCCAGCCCTATC (R)- GGGAAGTTCTGGCCAAAAGG	147	NM_133530
Matrix metalloproteinase 9 (Mmp9)	(F)- AAACATGCTGAAACCGGACC (R)- GAGGGATCATCTCGGCTACC	118	NM_031055
Glutathione S-transferase alpha 4 (Gsta4)	(F)- ACAGCTGGAGTGGAGTTTGA (R)- GTGTCAGTAGCATCCCGTCT	127	NM_001106840
Rap2 interacting protein (Rap2ip)	(F)- GCAGCATCGAGAACATGGAG (R)- TCTGGTAGTTCGGTTGTCCC	131	NM_198758
Tetraspanin 13 (Tspan13)	(F)- CGGAGAGTATGCTGGAGAGG (R)- TTCTCGTCAAAGGAAAGCGC	148	NM_001013244
Adrenomedullin (Adm)	(F)- ATGTTATTGGGTTCGCTCGC (R)- GGACGCTTGTAGTTCCCTCT	123	NM_012715
Spindle and kinetochore associated complex subunit 1 (Ska1)	(F)- GGCCAGAGGAGGATCTTGAG (R)- TCCTGACCTTGTGCTTGCTA	125	NM_001106134
Minichromosome maintenance complex component 10 (Mcm10)	(F)- GCATAACCTCCACTGGCATG (R)- ATTCCATCCCGTTCCCACTT	135	NM_001107366
Histone cluster 1, H1b (Hist1h1b)	(F)- GTCTCCCGCCAAGAAGAAGA (R)-GCCAATGCCTTCTTCAGAGC	147	NM_001109417
Integrin-binding sialoprotein (IBSP)	(F)- CAGTTATGGCACCACGACAG (R)- CATACTCAACCGTGCTGCTC	116	NM_012587
Transforming growth factor, beta 2 (TGFβ2)	(F)- TACCCGAGTCTAAGGTTGGC (R)-GGAAGGGACGAAGGACAGAA	123	BC100663
Bone morphogenic protein-4 (BMP-4)	(F)- CAAGCGTAGTCCCAAGCATC (R)- GGCCACGATCCAATCATTCC	115	NM_012827
Nestin	(F)- CTGCAGAAGAGGACCTGGAA (R)- CATCCACAGACCCTAGCGAT	129	NM_012987
Osteopontin (spp1)	(F)- CTGAAGCCTGACCCATCTCA (R)- TCGTCGTCATCATCGTCCAT	143	NM_012881

Table 1 Primer sequences used for primary rat pulp gene expression analyses

Gene	Gene name	Fold change	t-test with Storey	Up-regulation Reported Reference*
Rap2 interacting protein	Rap2ip	8.9	2.13E-05	
Glutathione S-transferase alpha 4	Gsta4	8.2	2.65E-04	Schroeder et al., 2007 Majumdar et al., 2012
Tubulin, beta 2B class IIb	Tubb2b	7.9	0.00234	LaBonte et al., 2009
Monoacylglycerol O-acyltransferase 2	Mogat2	7.1	0.006320	
Brain expressed, X-linked 1	Bex1	7.0	6.39E-04	Foltz et al., 2006 Fischer et al., 2007
Phospholamban	Pln	6.3	2.94E-06	
Transmembrane protein 35	Tmem35	5.1	6.32E-05	
Coronin, actin binding protein 1A	Coro1a	5.0	3.37E-04	Moore et al., 2004
Cell death-inducing DFFA-like effector a	Cidea	4.8	1.96E-04	
Tetraspanin 13	Tspan13	4.8	4.12E-04	
Pentraxin 3, long	Ptx3	4.6	0.01514	
Membrane-spanning 4-domains, subfamily A, member 14	Ms4a14	4.5	0.00328	
Kinesin family member C2	KIFC2	4.4	3.09E-04	
S100 calcium binding protein A1	S100a1	4.2	1.23E-04	Pryzbylkowski et al., 2008
Disabled homolog 1 (Drosophila)	Dab1	4.1	0.01277	Noh et al., 2009
Reticulon 1	Rtn1	4.1	4.72E-04	Fazi et al., 2009
Cyclohydrolase I feedback regulator	Gchfr	4.0	0.00414	
Angiopoietin-like 4	Angptl4	3.9	0.00126	Poulaki et al., 2009
Secretogranin V	Scg5	3.8	0.00139	Bracker et al., 2009
Integral membrane protein 2A	Itm2a	3.7	7.58E-04	
Alcohol dehydrogenase 1 (class I)	Adh1	3.7	7.58E-04	
Immunoglobulin superfamily, member 10	Igsf10	3.7	0.00171	
Adrenergic, beta-3-, receptor	Adrb3	3.6	0.00325	
GLI pathogenesis-related 1	Glipr1	3.6	3.49E-04	
Small nuclear ribonucleoprotein polypeptide N	Snrpn	3.6	0.01421	Suzuki et al., 2002
Uroplakin 1B	Upk1b	3.5	0.00587	Milutinovic et al., 2007
Chromobox homolog 7	Cbx7	3.4	0.00104	
Aldehyde oxidase 1	Aox1	3.4	8.74E-05	
Adrenomedullin	Adm	3.4	1.45E-05	Poulaki et al., 2009 Majumdar et al., 2012
CD302 molecule	Cd302	3.4	6.67E-04	
Brain expressed, X-linked 4	Bex4	3.3	0.00797	
Cholinergic receptor, muscarinic 4	Chrm4	3.3	7.30E-04	Ooi et al., 2006
SATB homeobox 1	Satb1	3.2	0.00794	
Tctex1 domain containing 1	Tctex1d1	3.2	0.00136	
Sulfite oxidase	Suox	3.2	9.10E-06	Lee et al., 2004
Cytochrome b-561	Cyb561	3.1	8.52E-04	
Ephrin1	Efna1	3.1	7.42E-05	Poulaki et al., 2009
Sphingosine-1-phosphate receptor 1	S1pr1	3.1	3.96E-04	Nguyen-Tran et al., 2014
Adrenergic, beta-2-, receptor, surface	Adrb2	3.0	7.36E-04	Foltz et al., 2006
Matrix metalloproteinase 9	Mmp9	3.0	4.46E-04	Mayo et al., 2003

Table 2 Top 40 known genes induced by SAHA in mineralizing rat DPC cultures at 24 h. References are for previous studies that reported up-regulation of the transcript or protein in cells or other cell systems by an HDACi (*).

Gene	Gene name	Fold change	t-test with Storey	Down-regulation Reported Reference*
Spindle and kinetochore associated complex subunit 1	Ska1	-97.2	1.12E-04	
Minichromosome maintenance complex component 10	Mcm10	-15.7	0.00957	Li and Li, 2008
DDB1 and CUL4 associated factor 15	Dcaf15	-15.2	0.00924	
MIS18 kinetochore protein homolog A (S. pombe)	Mis18a	-11.4	0.00919	
Stathmin 1	Stmn1	-10.1	0.00301	Milli et al., 2008
PDZ binding kinase	Pbk	-9.3	6.57E-04	
Cyclin A2	Ccna2	-8.7	4.30E-04	Schroeder et al., 2007 LaBonte et al., 2009, Majumdar et al., 2012 Koutsounas et al., 2013
Histone cluster 1, H1b	Hist1h1b	-7.8	3.17E-04	
Cyclin B1	Ccnb1	-7.6	0.00323	Schroeder et al., 2007
Kinesin family member 2C	Kif2c	-7.4	5.37E-05	Dudakovic et al., 2013
PHD finger protein 19	Phf19	-7.3	1.64E-04	
Antigen identified by monoclonal antibody Ki-67	Mki67	-7.1	2.43E-04	Majumdar et al., 2012 Liu et al., 2013
Microtubule-associated, homolog (Xenopus laevis)	Tpx2	-6.7	0.00401	
Ribonucleotide reductase M2	Rrm2	-6.7	0.01415	
Polo-like kinase 1	Plk1	-6.7	0.00152	Lee et al., 2004 Schroeder et al., 2007
Polo-like kinase 4	Plk4	-6.7	0.01458	Schroeder et al., 2007
Suppressor APC domain containing 2	Sapcd2	-6.7	1.32E-04	
Urocortin 2	Ucn2	-6.5	0.00291	
Topoisomerase (DNA) II alpha	Top2a	-6.3	0.00116	
Cell division cycle associated 3	Cdca3	-6.1	8.93E-04	Majumdar et al., 2012
Protein regulator of cytokinesis 1	Prc1	-6.1	0.00235	Majumdar et al., 2012
Ubiquitin-conjugating enzyme E2C	Ube2c	-6.1	0.00175	
IQ motif containing GTPase activating protein 3	Iqgap3	-6.0	0.01027	
Centromere protein F	Cenpf	-6.0	0.00641	
Sperm associated antigen 5	Spag5	-5.9	7.62E-04	
Cell division cycle 20 homolog (S. cerevisiae)	Cdc20	-5.8	0.00454	Majumdar et al., 2012
Microtubule associated serine/threonine kinase-like	Mastl	-5.8	0.00195	
Kinesin family member C1	Kifc1	-5.7	1.38E-04	
Asp (abnormal spindle) homolog, microcephaly associated (Drosophila)	Aspm	-5.7	0.00153	Dudakovic et al., 2013
Epithelial cell transforming sequence 2 oncogene	Ect2	-5.7	9.54E-04	
Centrosomal protein 55	Cep55	-5.6	0.00190	
Kinesin family member 20B	Kif20b	-5.6	0.00303	
Protein regulator of cytokinesis 1	Prc1	-5.6	4.66E-04	
Kinesin family member 20A	Kif20a	-5.5	0.00222	LaBonte et al., 2009, Majumdar et al., 2012
Ubiquitin-conjugating enzyme E2T (putative)	Ube2t	-5.4	8.76E-04	Schroeder et al., 2007
MMS22-like, DNA repair protein	Mms22l	-5.4	2.01E-04	
ASF1 anti-silencing function 1 homolog B (S. cerevisiae)	Asf1b	-5.4	0.00170	
GINS complex subunit 1 (Psf1 homolog)	Gins1	-5.3	4.08E-04	
Transforming, acidic coiled-coil containing protein	Tacc3	-5.3	0.00238	
Rattus norvegicus histone cluster 2, H3c2	Hist2h3c2	-5.2	3.40E-05	

Table 3 Top 40 known genes suppressed by SAHA in mineralizing rat DPC cultures at 24 h. References are for previous studies that reported down-regulation of the transcript or protein in cells or other cell systems by an HDACi (*).

Gene	Gene name	Fold change	t-test with Storey	Up-regulation Reported Reference*
Inositol polyphosphate-4-phosphatase, type II	Inpp4b	3.7	0.00732	
Disabled homolog 1 (Drosophila)	Dab1	3.6	0.00163	Koutsounas et al., 2013
BCL2 interacting protein harakiri	Hrk	2.9	0.00391	
T-cell differentiation protein 2	Mal2	2.8	0.00442	
Glutamate receptor, ionotropic, kainate 4	Grik4	2.8	0.00484	
Aquaporin 3	Aqp3	2.5	9.34E-04	
Purinergic receptor P2X, ligand-gated ion channel, 2	P2rx2	2.4	0.00207	
RAS guanyl releasing protein 3 (calcium and DAG-regulated)	Rasgrp3	2.3	0.00204	Moore et al., 2004
Solute carrier organic anion transporter family, member 4a1	Slco4a1	2.1	0.00696	
Agmatine ureohydrolase (agmatinase)	Agmat	2.1	0.00548	
Catenin (cadherin-associated protein), delta 2	Ctnnd2	2.0	0.00436	
Cd5 molecule-like	Cd5l	2.0	0.00124	
Coiled-coil domain containing 67	Ccdc67	1.9	0.00276	
Prolyl 4-hydroxylase, alpha polypeptide I	P4ha1	1.9	0.00242	
S100 calcium binding protein A11 (calizzarin)	S100a11	1.9	9.81E-04	
Ameloblastin	Ambn	1.9	5.35E-04	
Tenascin C	Tnc	1.8	0.0014	
EF-hand domain family, member D1	Efhd1	1.8	6.01E-04	
Thy-1 cell surface antigen	Thy1	1.8	2.52E-04	
Cytoplasmic FMR1 interacting protein 2	Cyfip2	1.8	0.00417	

Table 4 Top 20 known genes induced by SAHA in mineralizing rat DPC cultures at 14 days. References are for previous studies that reported up-regulation of the transcript or protein in cells or other cell systems by an HDACi.

Gene	Gene name	Fold change	t-test with Storey	Downegulation Reported Reference*
Keratin 18	Krt18	-2.8	0.001	
Olfactory receptor 1749	Olr1749	-2.5	2.96E-04	
Eph receptor A3	Epha3	-2.4	0.008	Poulaki et al., 2009
G protein-coupled receptor 137C	Gpr137c	-2.1	0.00265	
Vomeronasal 1 receptor 68	Vom1r68	-2.1	0.00598	
Myosin light chain kinase	Mylk	-2.0	0.00359	
Olfactory receptor 777	Olr777	-1.9	0.00885	
G-protein signalling 4	Rgs4	-1.9	0.002	
Interphotoreceptor matrix proteoglycan 1	Impg1	-1.9	0.00428	
Transmembrane 4 L six family member 20	Tm4sf20	-1.9	4.37E-04	
Somatostatin receptor 2	Sstr2	-1.9	0.00214	
Forkhead box A3	Foxa3	-1.9	0.00163	
Purkinje cell protein 4 , transcript variant 1	Pcp4	-1.9	0.00311	
Aldehyde dehydrogenase 1 family, member A2	Aldh1a2	-1.9	0.00668	
Zinc finger and BTB domain containing 38	Zbtb38	-1.8	0.00175	
Upper zone of growth plate and cartilage matrix associated	Ucma	-1.8	6.97E-04	
Cytochrome P450, family 4, subfamily a, polypeptide 8	Cyp4a8	-1.8	0.00131	
Leucine rich repeat neuronal 2	Lrm2	-1.8	0.00422	
Signal transducer and activator of transcription 6	Stat6	-1.8	0.00733	
Protamine 2 (Prm2)	Prm2	-1.8	0.00151	
Insulin-like growth factor binding protein 3	Igfgp3	-1.8	1.38E-04	

Table 5 Top 20 known genes suppressed by SAHA in mineralizing rat DPC cultures at 14 days. References are for previous studies that reported down-regulation of the transcript or protein in cells or other cell systems by an HDACi (*).

Gene	Number changed	% changed	z-score	PermuteP
Cell cycle	17	39	11.9	0.0001
DNA Replication	11	41	9.8	0.0001
G1 to S cell cycle control	13	31	9.0	0.0001
Mismatch repair	3	50	5.75	0.0005
Homologous recombination	4	36	5.48	0.0005
Hedgehog Signalling Pathway	3	25	3.71	0.0035
Matrix Metalloproteinases*	3	16.7	2.75	0.0085
Endochondral Ossification*	4	12.9	2.55	0.0085

Table 6 Over-represented pathways (genes > 2 fold) at 24h, analysed using GoElite software. In order to remove falsely over-represented pathways results were filtered by the number genes changed (>2), Z Score (>1.96), and PermuteP (<0.05). These pruned results minimize redundant terms and pathways. Over-represented upregulated pathways marked with asterisk (*).

Table 7 A comparison of cDNA gene expression microarray and validatory qRT-PCR at 24 h and 14 days. n=4 for both sets of experiments.

Gene	Fold change cDNA microarray (24h)	Fold change RT-PCR (24h)
Adm	3.4	3.06
BMP-4	1.9	2.79
Dab1	4.13	5.17
Gsta4	8.21	14.5
Hist1h1b	-7.83	-13.0
IBSP	2.2	2.38
Krt18	-2.8	-2.75
Mcm10	15.72	-14.3
Mmp9	3.0	2.76
Mmp13	2.45	2.19
Nestin	1.1	1.82
Rap2ip	8.9	14.91
Rasgrp3	1.3	1.15
Ska1	-97.2	-72.5
TGFβ2	2.78	3.76
Tspan13	4.84	6.35
Gene	Fold change cDNA microarray (14d)	Fold change RT-PCR (14d)
Ambn	1.88	1.72
Epha3	-2.4	-2.06
Krt18	-2.8	-2.65
Mal2	2.83	2.73
Mmp13	1.61	1.05
Rasgrp13	2.33	2.32
Spp-1	1.1	1.29
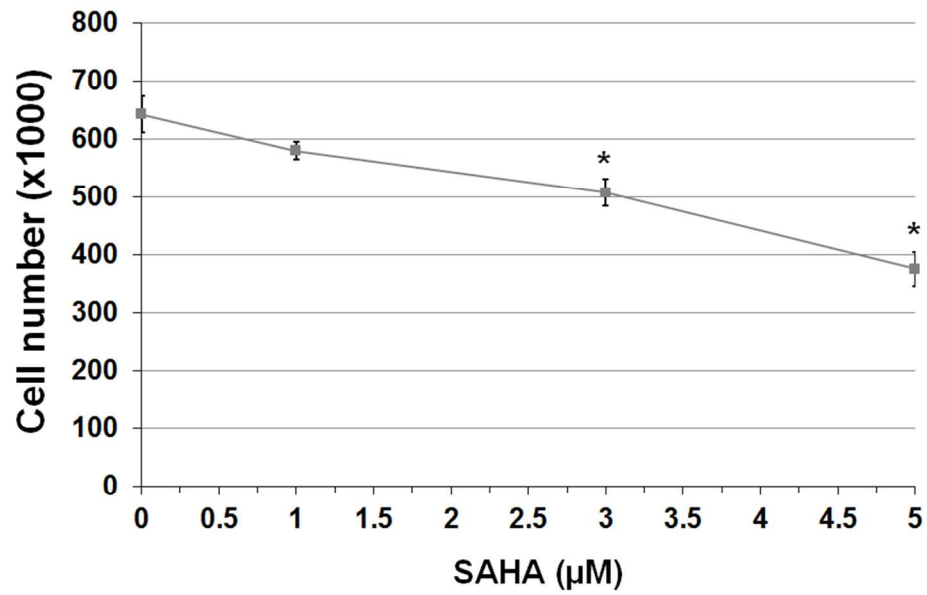
Fig. 1A
255x156mm (96 x 96 DPI)
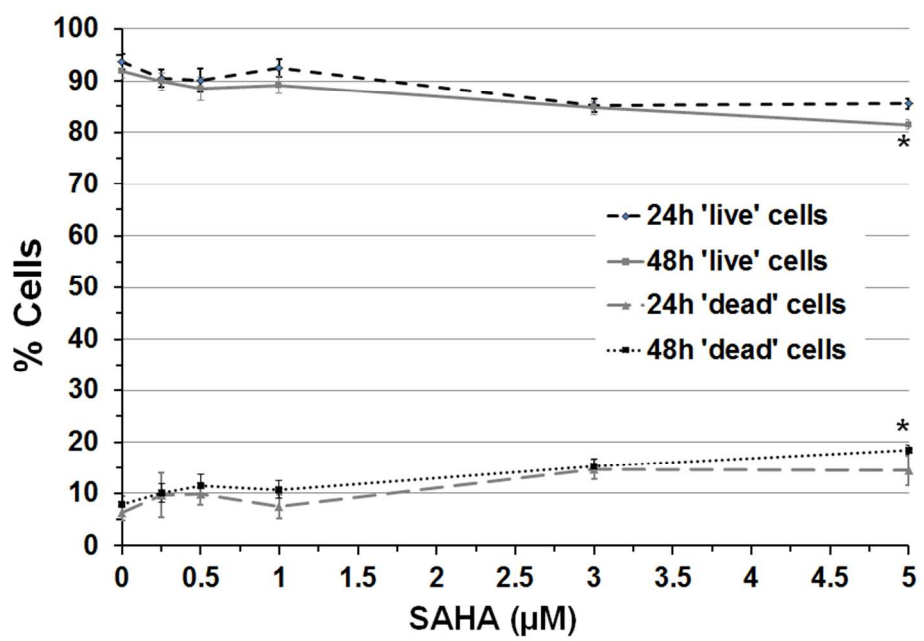
Fig. 1B
258x168mm (96 x 96 DPI)
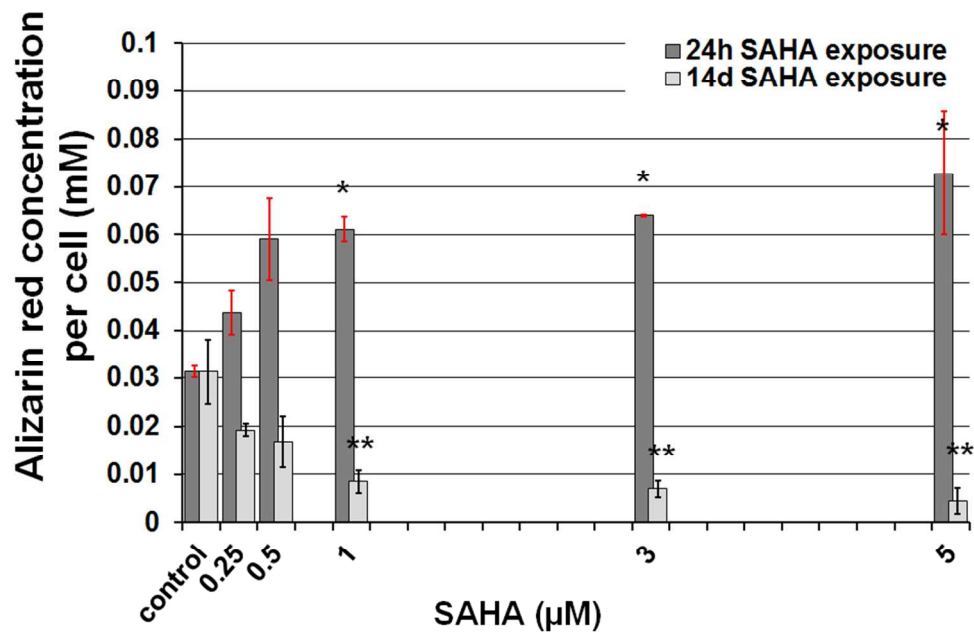
Fig. 1C
258x169mm (96 x 96 DPI)
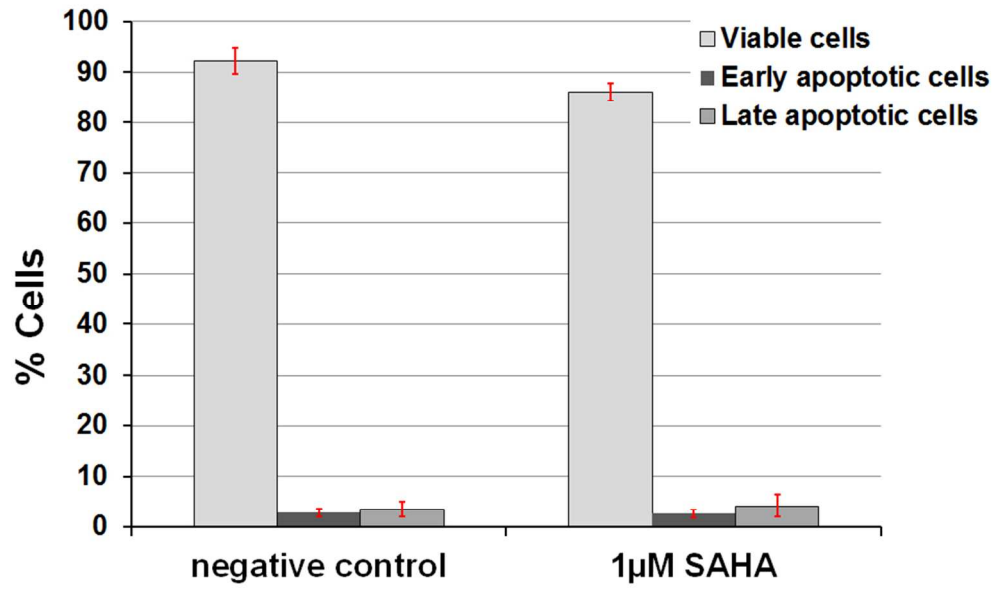
Fig. 1D
255x156mm (96 x 96 DPI)
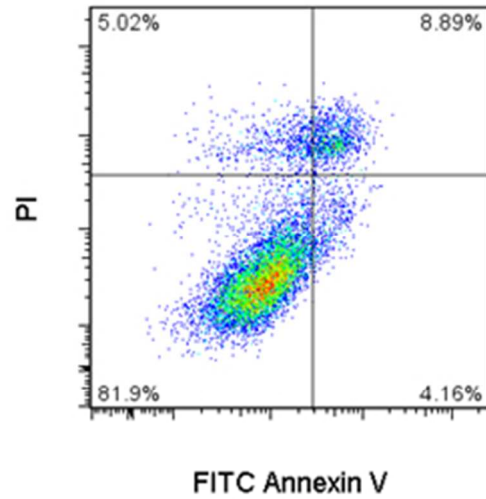
Fig. 1E
91x81mm (96 x 96 DPI)
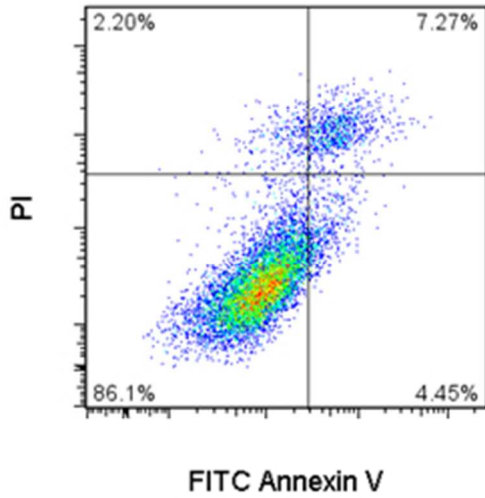
Fig. 1F
91x81mm (96 x 96 DPI)
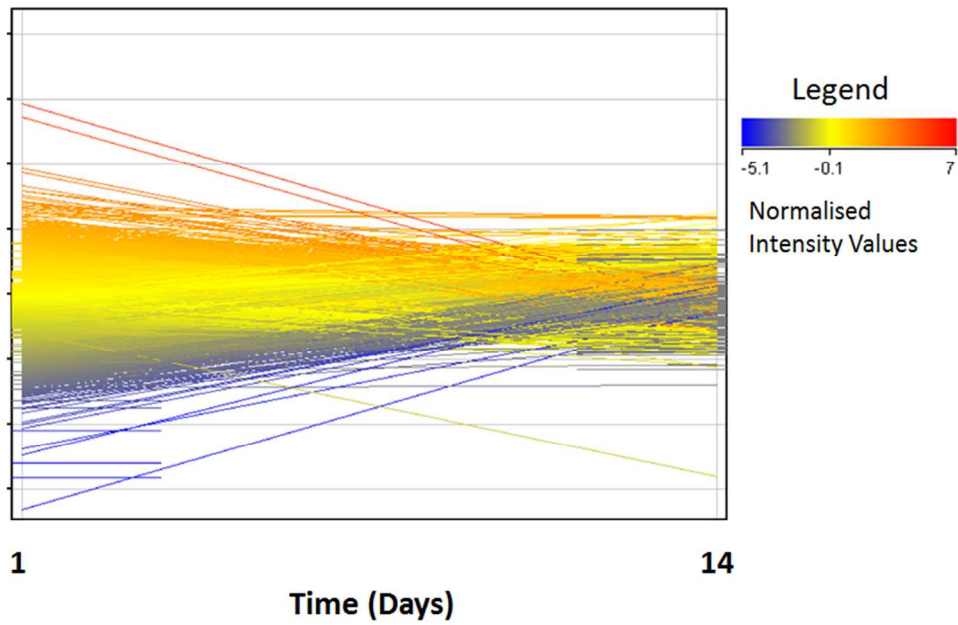
Fig. 2A
227x149mm (96 x 96 DPI)

Time point of microarray	Total number of genes	Up-regulated	Down-regulated	Genes altered as % of total genes present (23347)
24 hours	764	314	450	3.3%
14 days	36	23	13	0.15%

Fig. 2B
183x38mm (96 x 96 DPI)
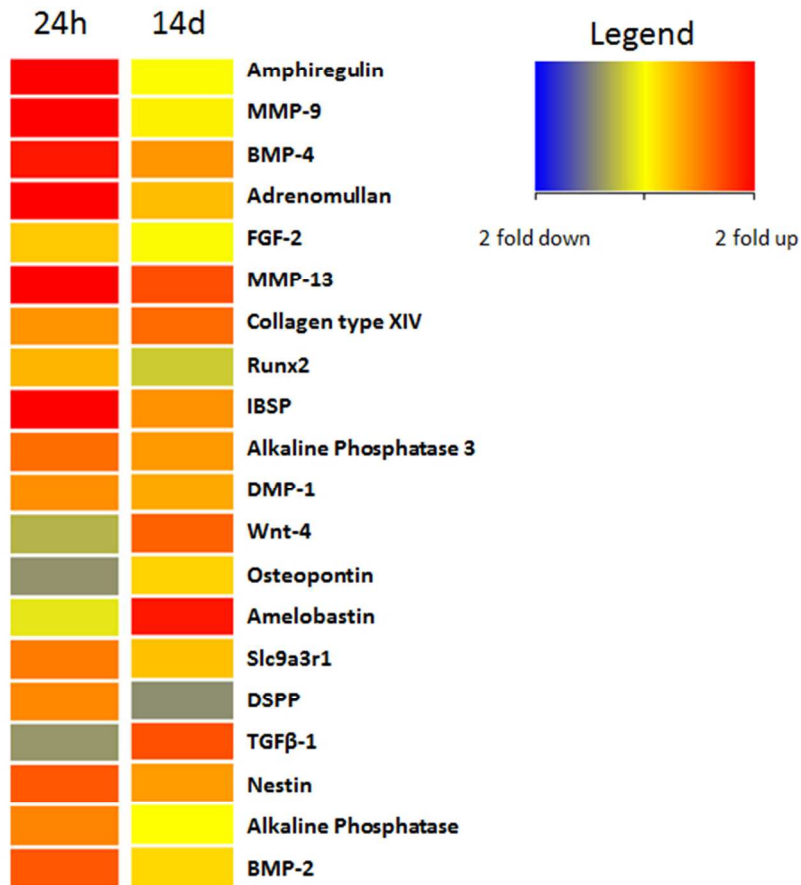
Fig. 2C
177x166mm (96 x 96 DPI)
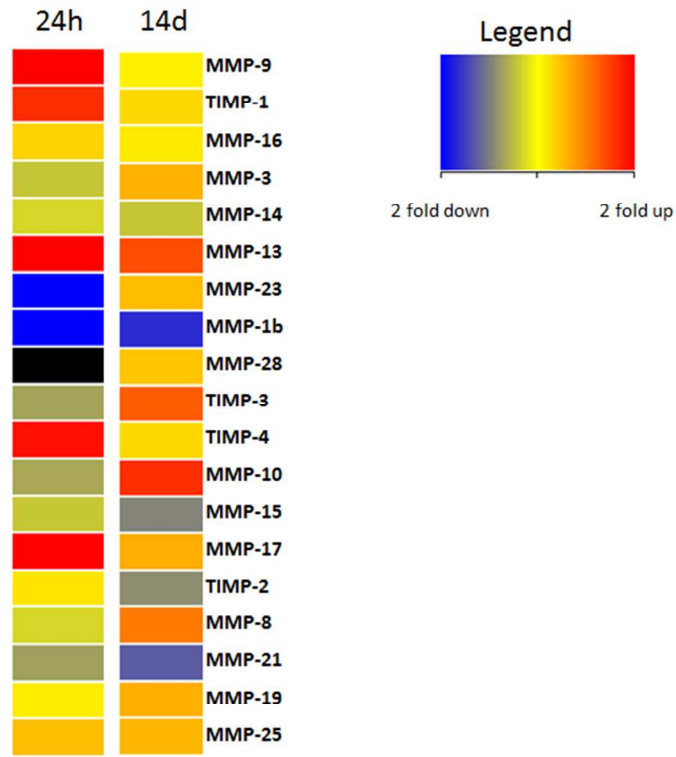
Fig. 2D
200x160mm (96 x 96 DPI)
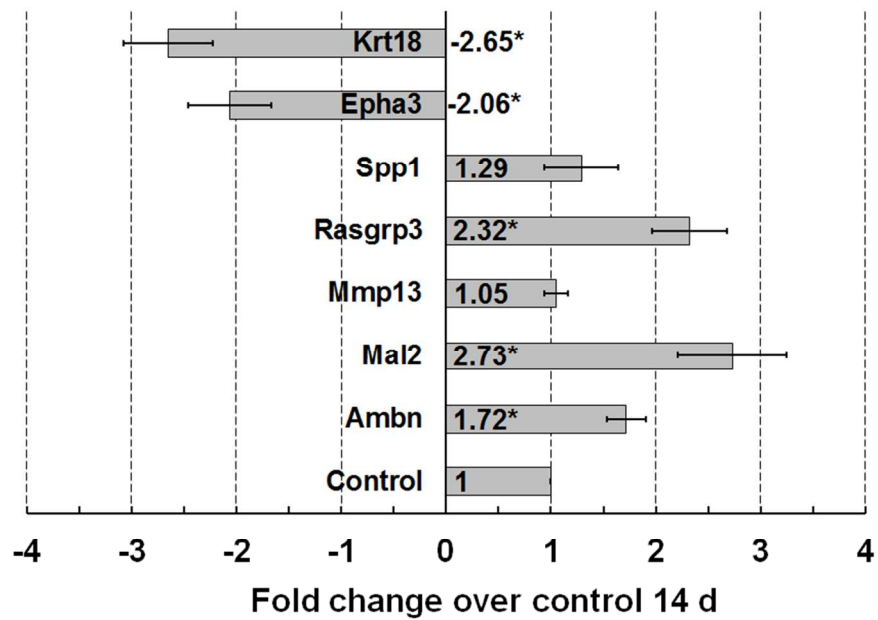
Fig. 3A
258x169mm (96 x 96 DPI)

1
2
3
4
5
6
7
8
9
10
11
12
13
14
15
16
17
18
19
20
21
22
23
24
25
26
27
28
29
30
31
32
33
34
35
36
37
38
39
40
41
42
43
44
45
46
47
48
49
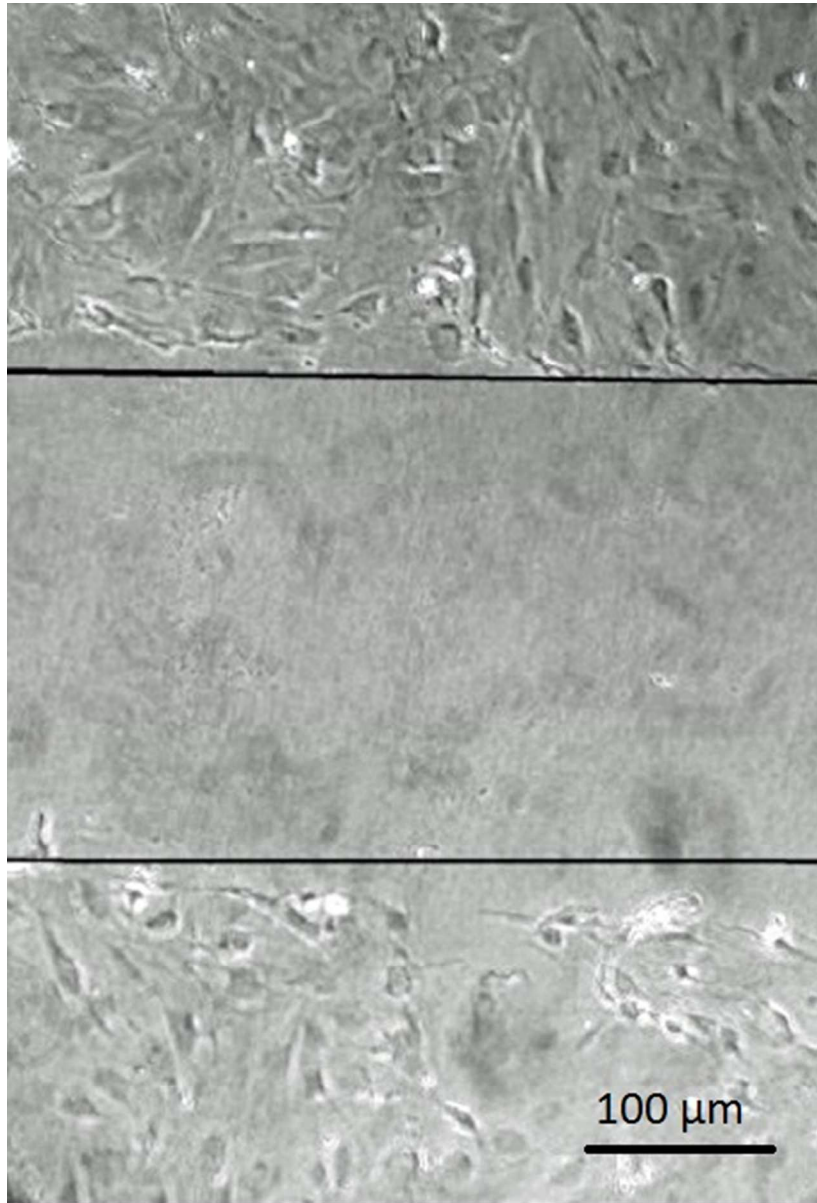50
51
52
53
54
55
56
57
58
59
60
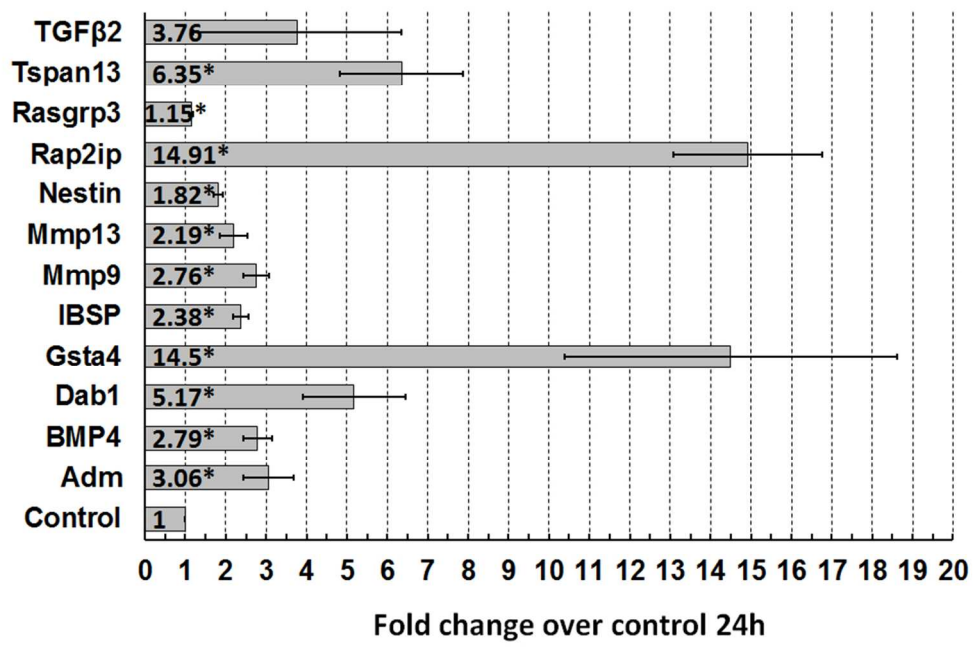
Fig. 3B
258x169mm (96 x 96 DPI)
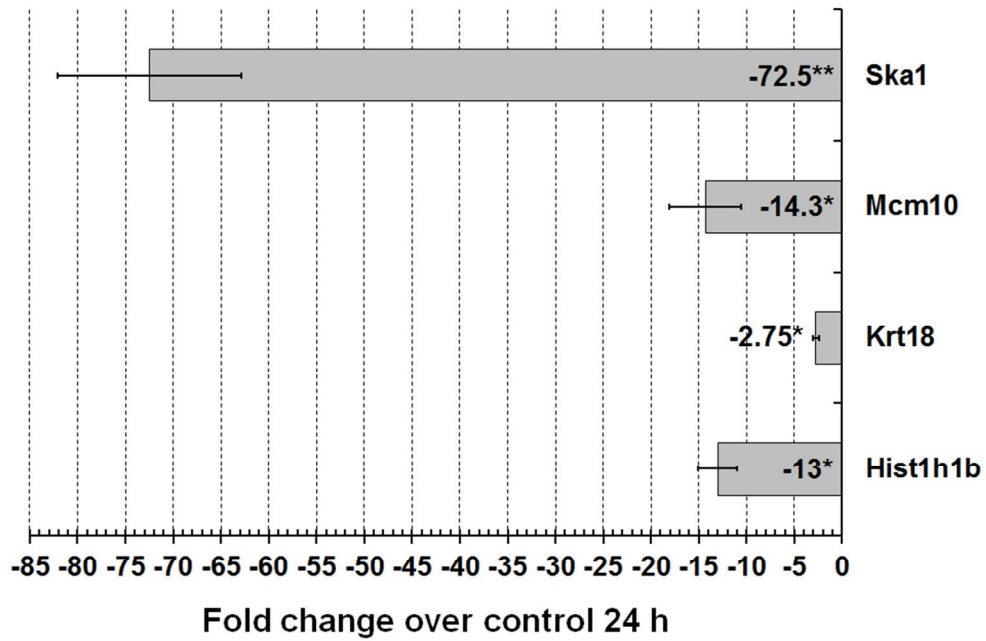
Fig. 3C
258x169mm (96 x 96 DPI)
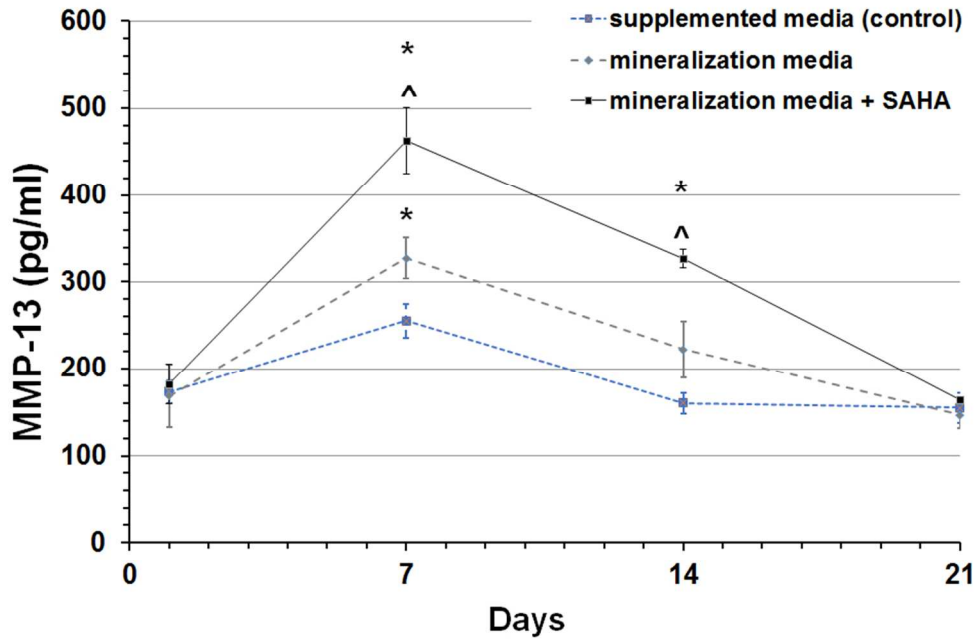
Fig. 4A
257x168mm (96 x 96 DPI)
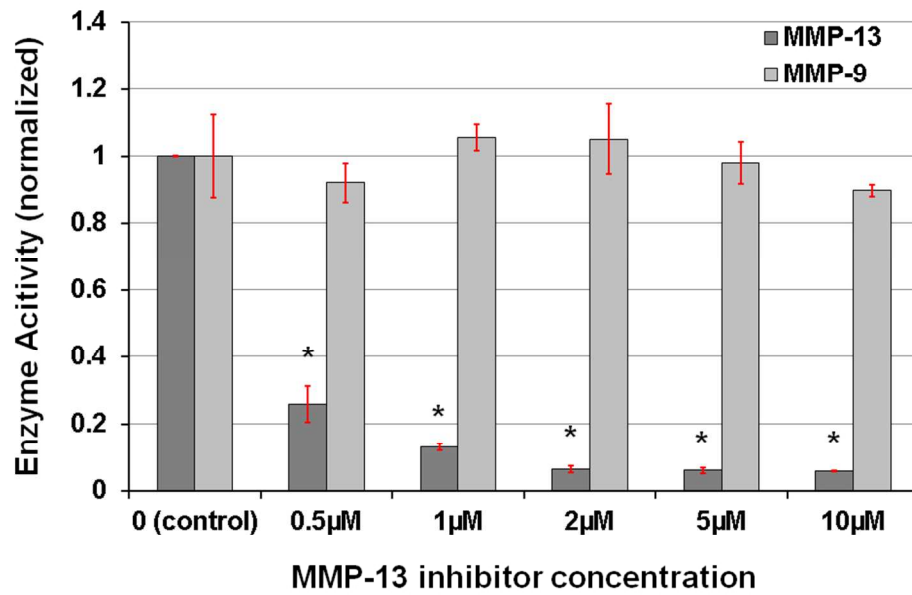
Fig. 4B
272x176mm (96 x 96 DPI)
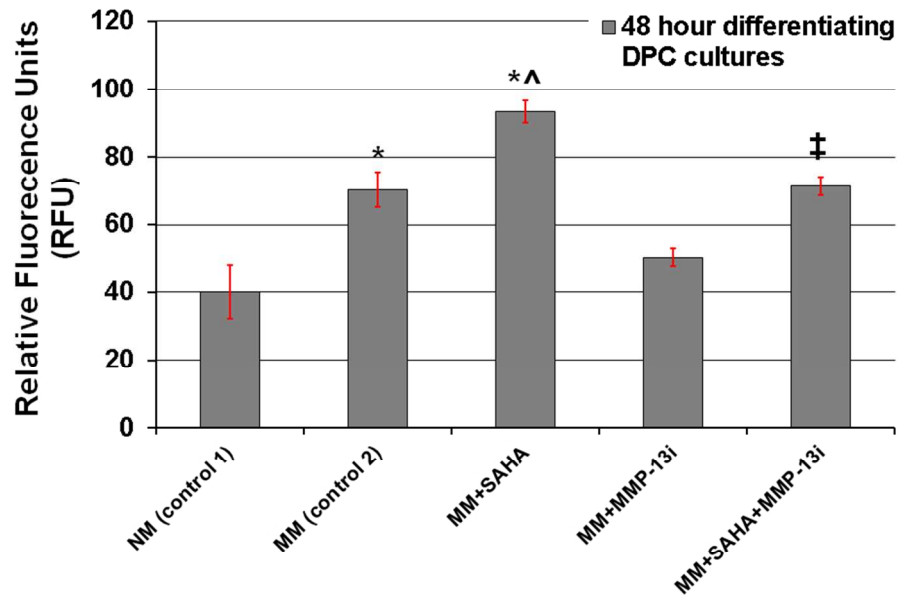
1
2
3
4
5
6
7
8
9
10
11
12
13
14
15
16
17
18
19
20
21
22
23
24
25
26
27
28
29
30
31
32
33
34
35
36
37
38
39
40
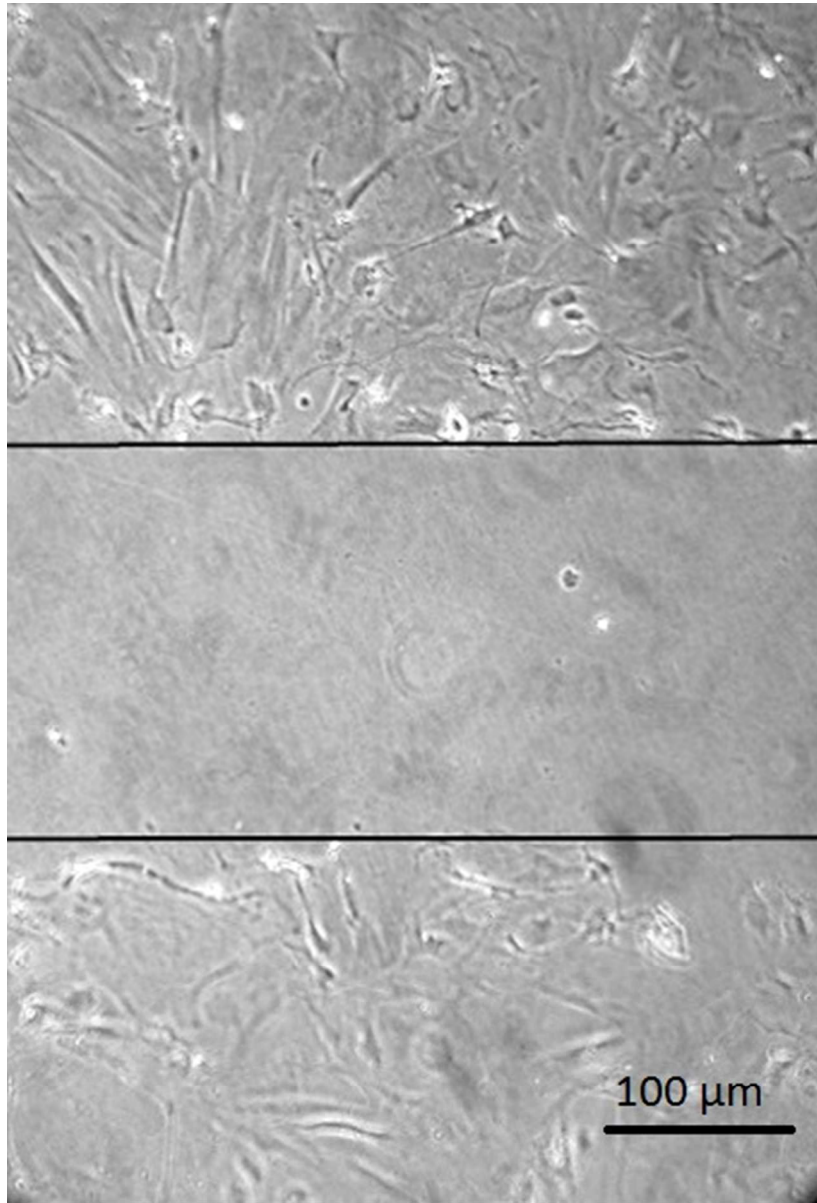41
42
43
44
45
46
47
48
49
50
51
52
53
54
55
56
57
58
59
60

Fig. 4C
272x176mm (96 x 96 DPI)
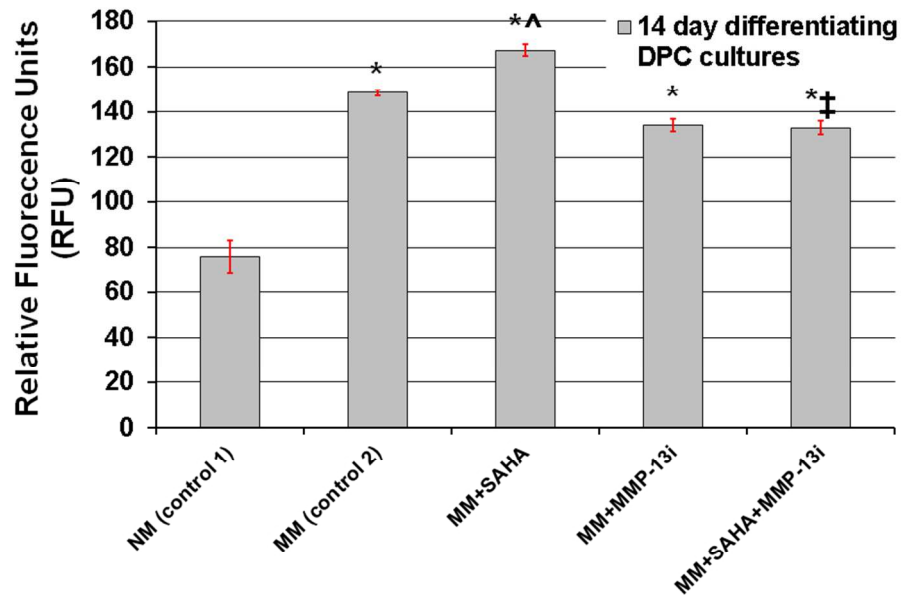
Fig. 4D
272x176mm (96 x 96 DPI)
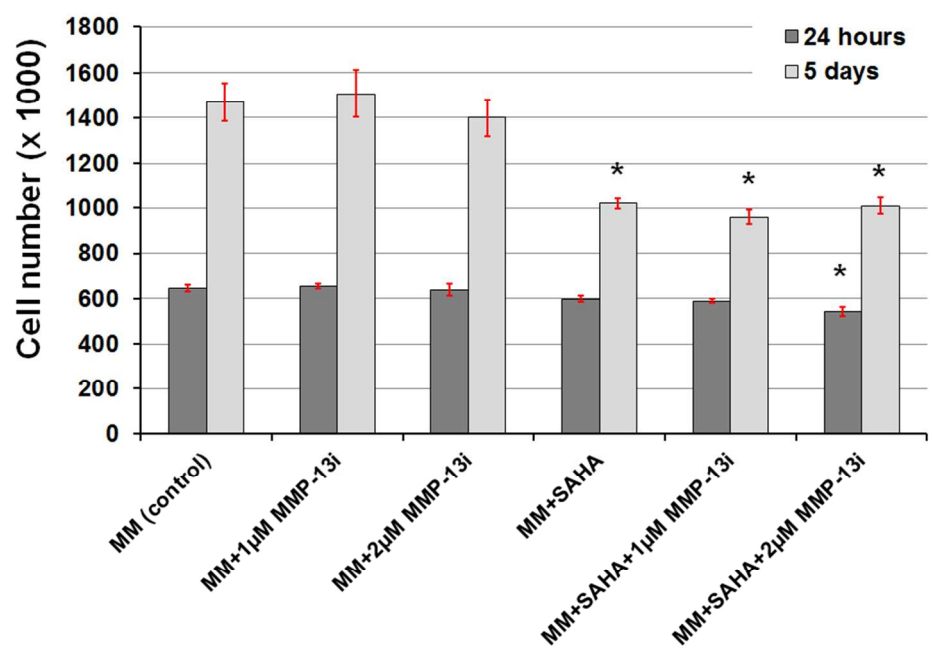
Fig. 5A
258x169mm (96 x 96 DPI)
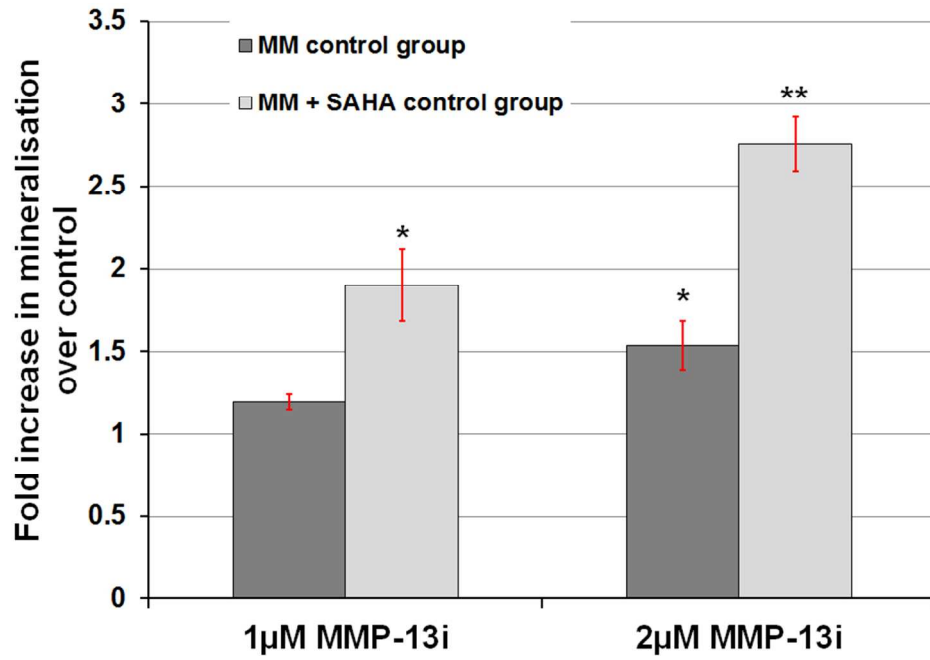
Fig. 5B
257x169mm (96 x 96 DPI)
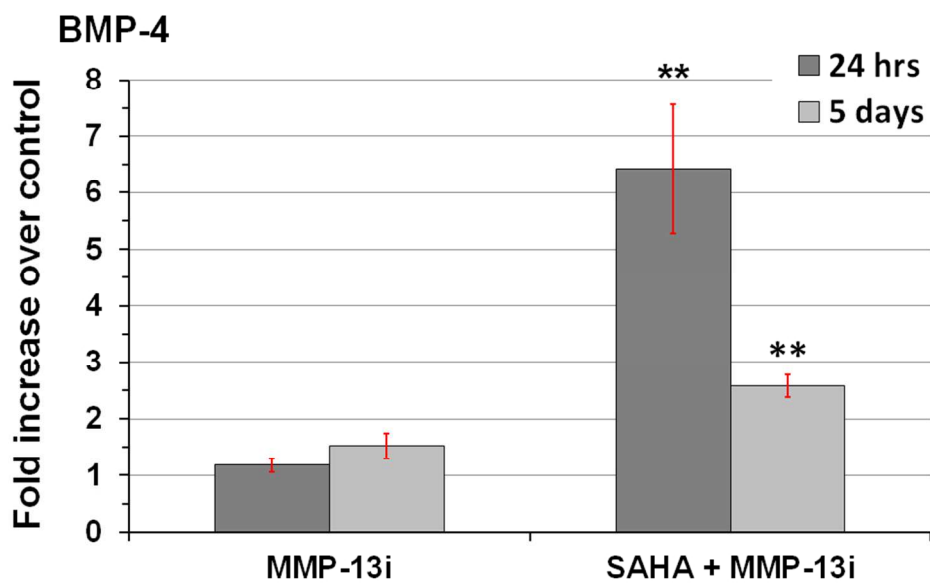
Fig. 5Ci
272x176mm (96 x 96 DPI)
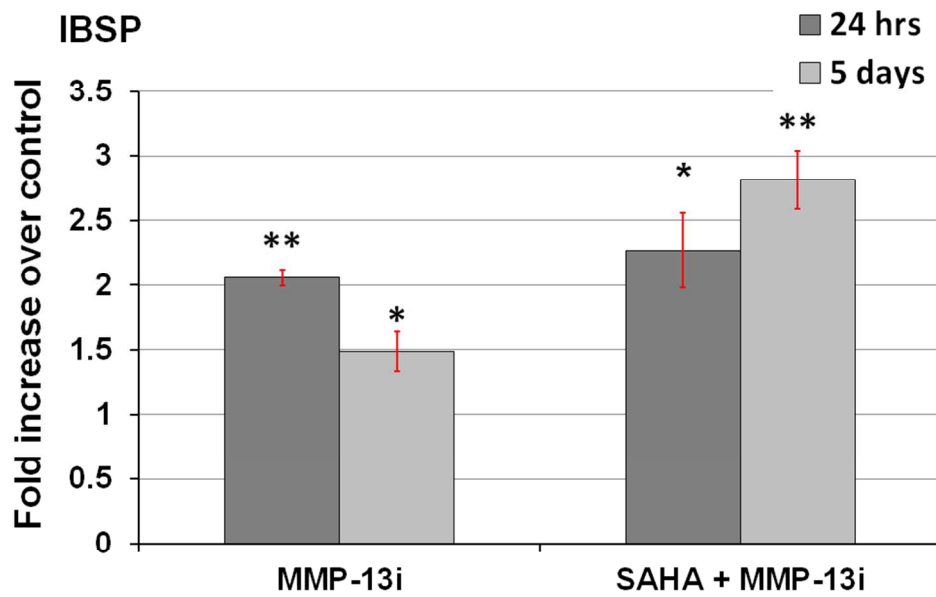
Fig. 5Cii
272x176mm (96 x 96 DPI)
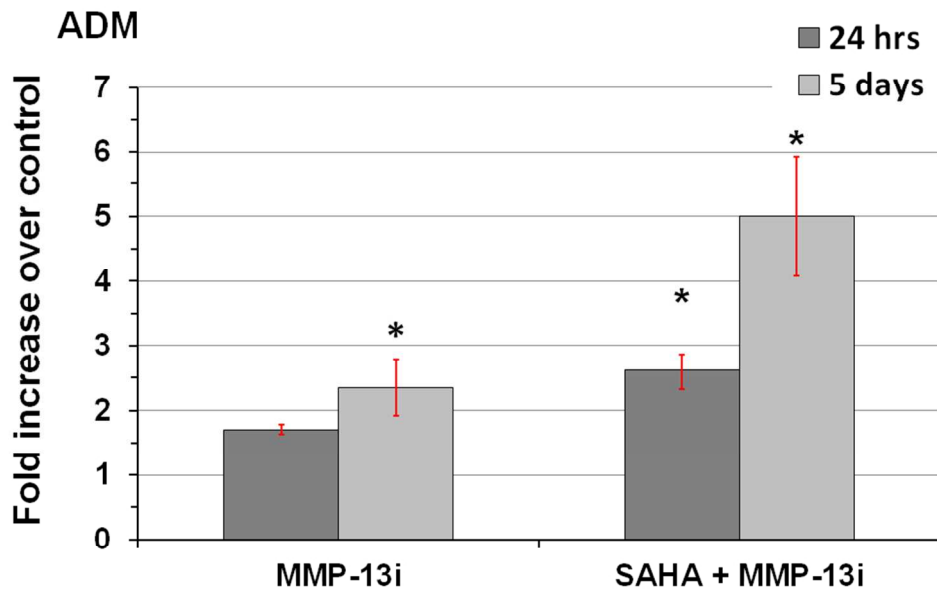
Fig. 5Ciii
272x176mm (96 x 96 DPI)
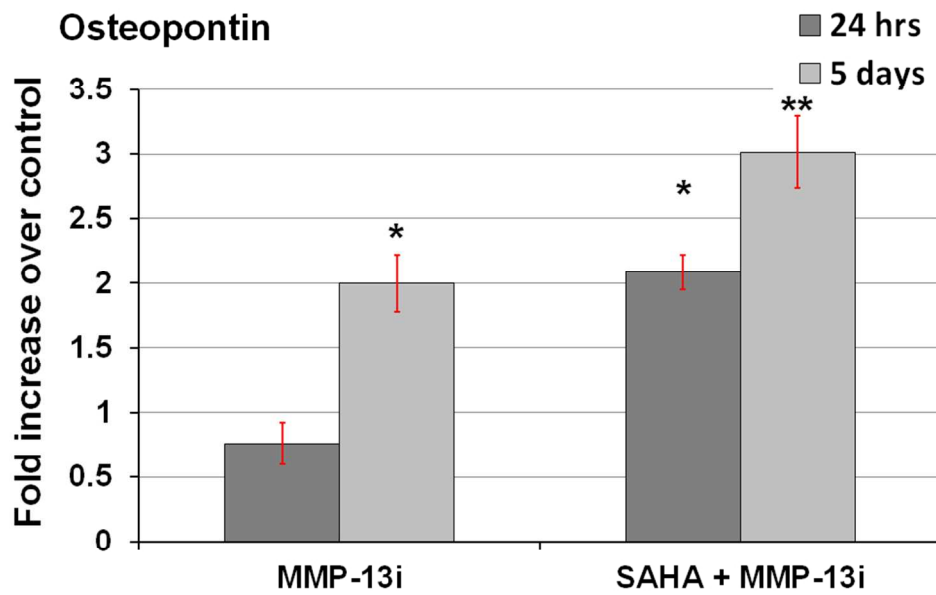
Fig. 5Civ
272x176mm (96 x 96 DPI)
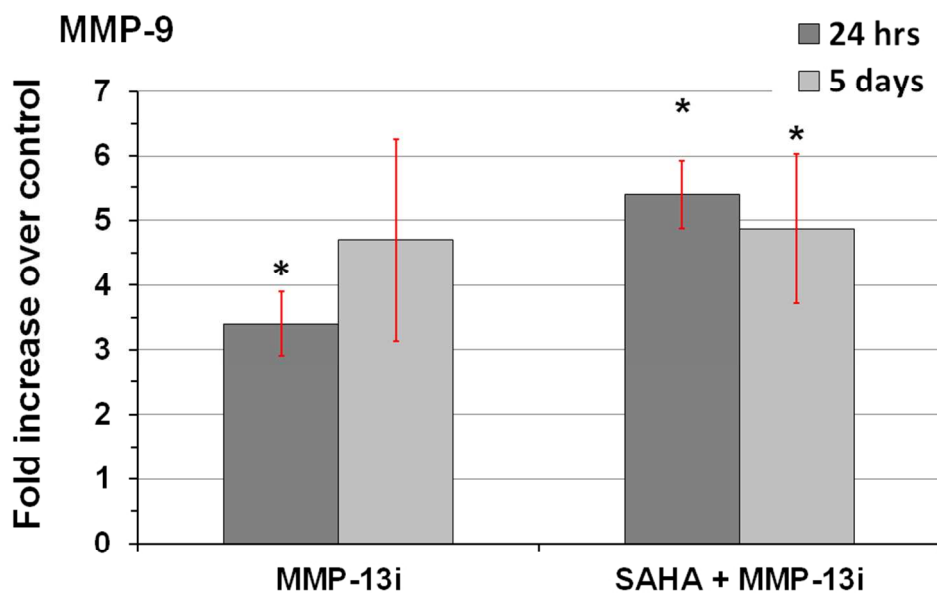
Fig. 5Cv
272x176mm (96 x 96 DPI)
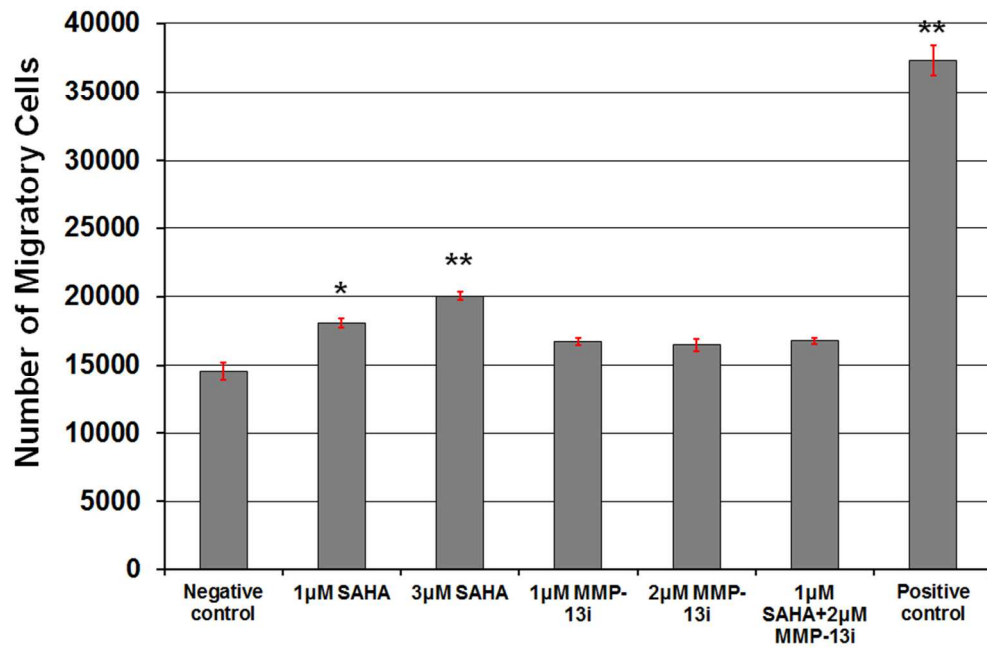
Fig. 6A
258x169mm (96 x 96 DPI)

Fig. 6B
272x176mm (96 x 96 DPI)
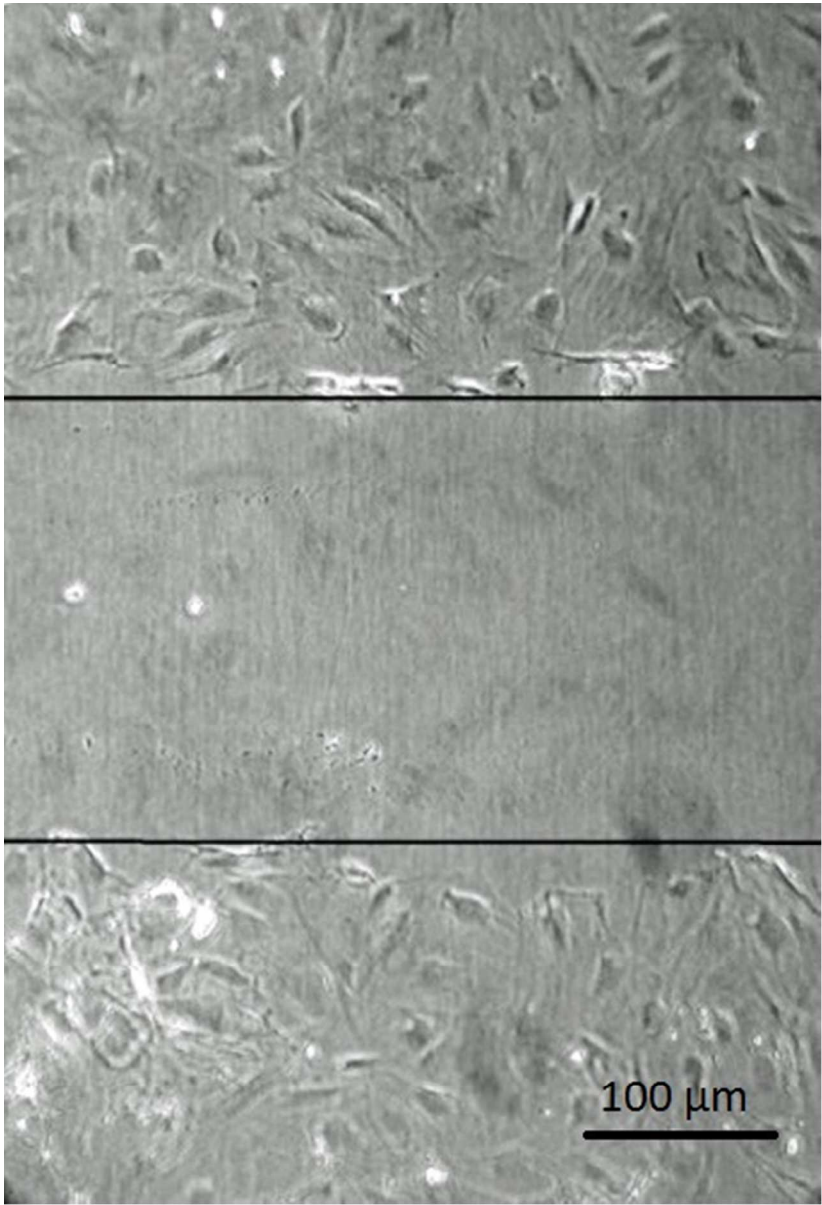
Fig. 6Ci
39x57mm (300 x 300 DPI)

Fig. 6Cii
39x57mm (300 x 300 DPI)

Fig. 6Ciii
39x57mm (300 x 300 DPI)

1
2
3
4
5
6
7
8
9
10
11
12
13
14
15
16
17
18
19
20
21
22
23
24
25
26
27
28
29
30
31
32
33
34
35
36
37
38
39
40
41
42
43
44
45
46
47
48
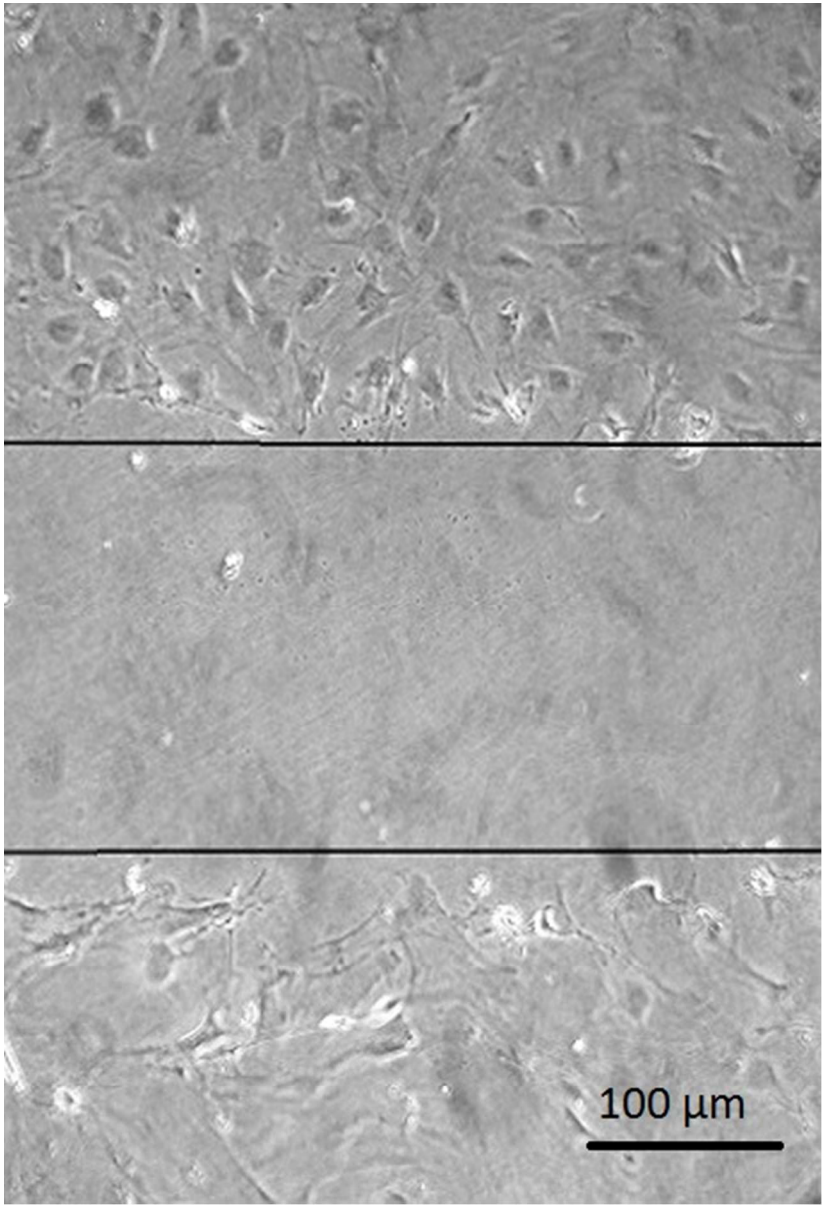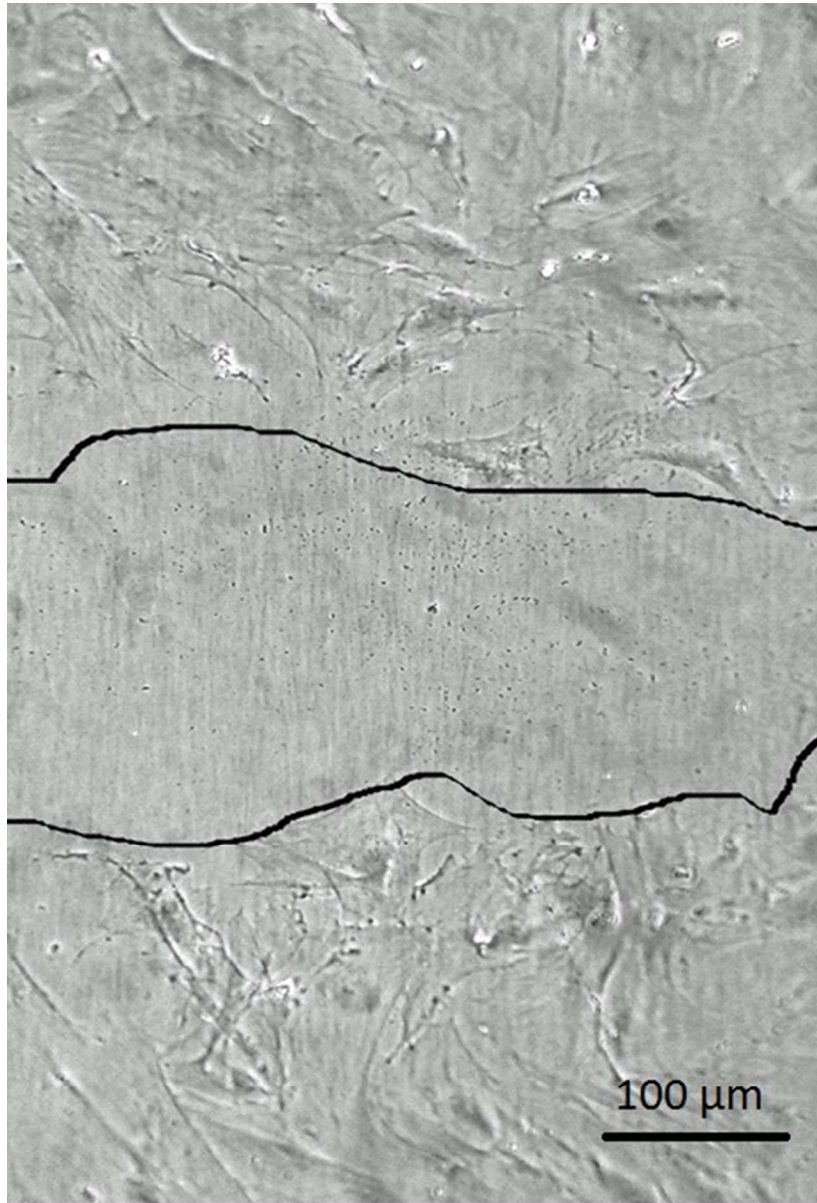49
50
51
52
53
54
55
56
57
58
59
60

Fig. 6Civ
39x57mm (300 x 300 DPI)

Fig. 6Di
39x57mm (300 x 300 DPI)

Fig. 6Dii
39x57mm (300 x 300 DPI)

Fig. 6Diii
39x57mm (300 x 300 DPI)

1
2
3
4
5
6
7
8
9
10
11
12
13
14
15
16
17
18
19
20
21
22
23
24
25
26
27
28
29
30
31
32
33
34
35
36
37
38
39
40
41
42
43
44
45
46
47
48
49
50
51
52
53
54
55
56
57
58
59
60

Fig. 6Div
39x57mm (300 x 300 DPI)

1
2
3
4
5
6
7
8
9
10
11
12
13
14
15
16
17
18
19
20
21
22
23
24
25
26
27
28
29
30
31
32
33
34
35
36
37
38
39
40
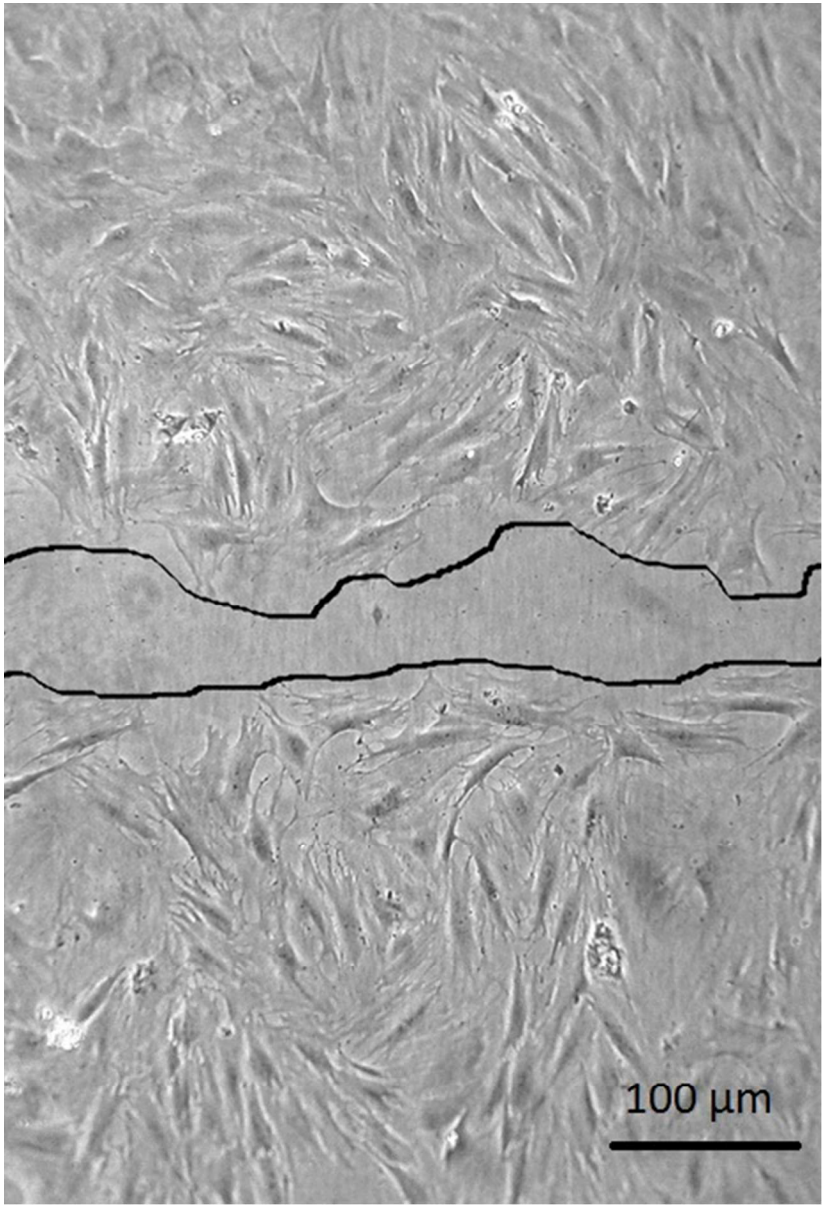41
42
43
44
45
46
47
48
49
50
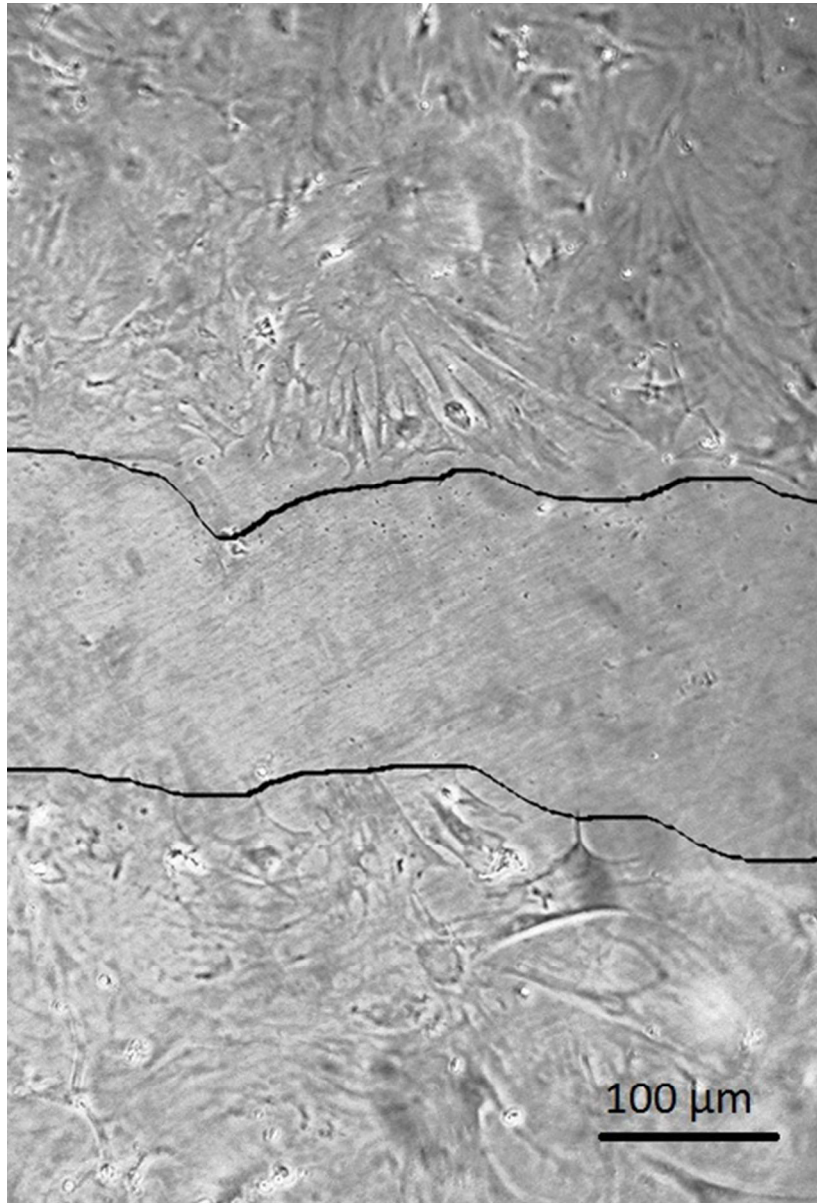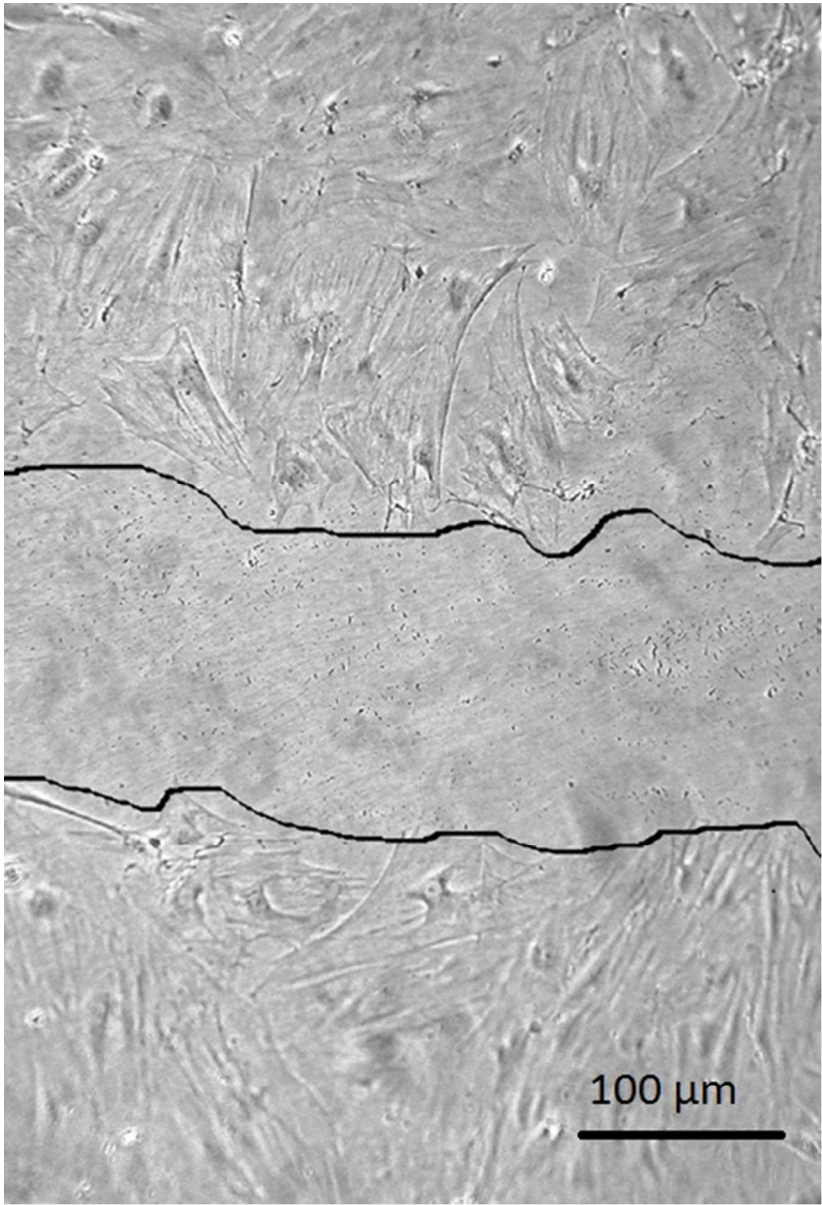51
52
53
54
55
56
57
58
59
60

HEALTHY TOOTH

TOOTH WITH PULP EXPOSURE

A. New generation of odontoblast-like cells and mineralisation stimulated by SAHA application

B. HDACi-induced MMP-13 expression↑↑ in pulp cells. MMP-13 organises dentine bridge formation, pulp matrix remodelling and releases/activates growth factors for angiogenesis and repair

C. Extracellular matrix proteins released from dentine activated by MMPs (including MMP-13) to stimulate repair precesses

Stem/progenitor cell recruitment stimulated by MMP-13

⚝ Odontoblast-like cell
● Progenitor/stem cell
🩸 Blood vessels
〰 Dentine matrix proteins

Low basal MMP-13 expression in health

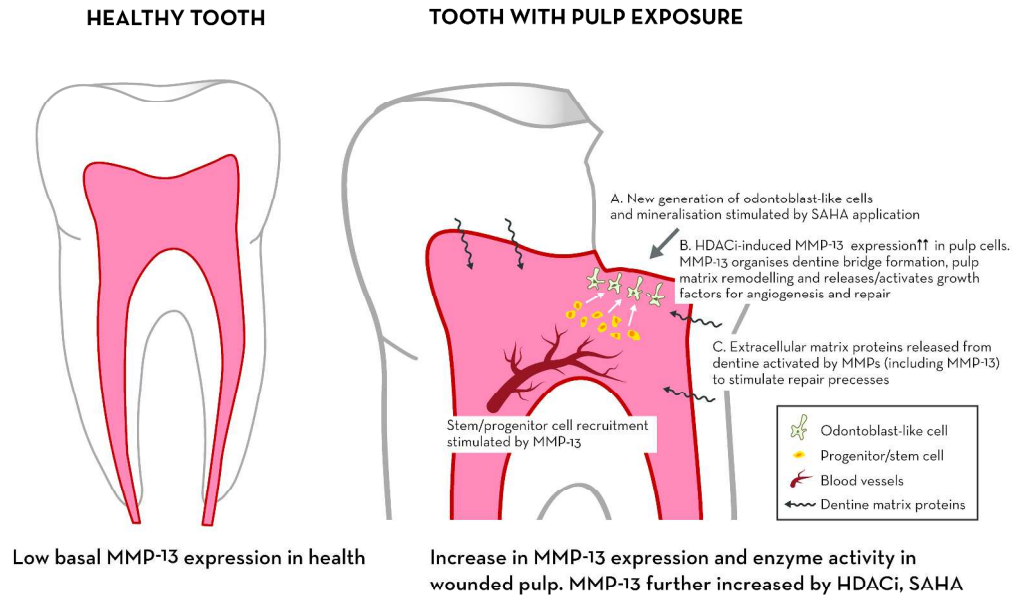Increase in MMP-13 expression and enzyme activity in wounded pulp. MMP-13 further increased by HDACi, SAHA

Fig. 7
286x221mm (300 x 300 DPI)